International Journal of Bifurcation and Chaos, Vol. 24, No. 2 (2014) 1450024 (30 pages)

DOI: 10.1142/S0218127414500242

# Codimension-2 Border Collision Bifurcations in One-Dimensional Discontinuous Piecewise Smooth Maps

Laura Gardini[†] and Viktor Avrutin[*,‡]
*DESP, University of Urbino, Italy*
[*]*IST, University of Stuttgart, Germany*
[†]*Laura.Gardini@uniurb.it*
[‡]*Avrutin.Viktor@ist.uni-stuttgart.de*

Irina Sushko
*Institute of Mathematics,*
*National Academy of Sciences of Ukraine, Ukraine*
*Sushko@imath.kiev.ua*

Received August 10, 2013; Revised October 30, 2013

We consider a two-parametric family of one-dimensional piecewise smooth maps with one discontinuity point. The bifurcation structures in a parameter plane of the map are investigated, related to codimension-2 bifurcation points defined by the intersections of two border collision bifurcation curves. We describe the case of the collision of two stable cycles of any period and any symbolic sequences. For this case, we prove that the local monotonicity of the functions constituting the first return map defined in a neighborhood of the border point at the parameter values related to the codimension-2 bifurcation point determines, under suitable conditions, the kind of bifurcation structure originating from this point; this can be either a period adding structure, or a period incrementing structure, or simply associated with the coupling of colliding cycles.

*Keywords*: Border collision bifurcations; codimension-2 bifurcations; one-dimensional maps; piecewise smooth maps; discontinuous maps.

## 1. Introduction

Piecewise smooth maps are well-known to show several phenomena which cannot occur in smooth systems. The most characteristic are *border collision bifurcations* (BCB for short) occurring when a point of a cycle collides (under parameter variation) with a border point which separates different definition regions of the system. Such a collision may be associated with the disappearance of the cycle and may lead to a drastic change in the dynamic behavior, as for example, to a direct transition from an attracting cycle to a chaotic attractor (see [Nusse & Yorke, 1992; di Bernardo *et al.*, 1999]).

An important feature of 1D maps with one discontinuity point regards the occurrence of codimension-2 BCBs. In fact, when dealing with a *two-dimensional parameter plane* of a *discontinuous map* one can observe particular points at which two BCB curves, related to BCBs of two different cycles, intersect transversely. These points are of great interest, because in many cases they represent so-called *organizing centers* giving rise to different complex bifurcation structures [Avrutin *et al.*, 2007; Gardini *et al.*, 2012]. In this paper we consider a codimension-2 BCB point $\mathcal{B}$, which corresponds to the simultaneous collision of two attracting cycles

with the border point from its opposite sides, i.e. a point of one cycle collides with the border point from the left and a point of the other cycle from the right.[1] As we show, at point $\mathcal{B}$ the first return map defined in a neighborhood of the border point is continuous in the border point, which also represents a fixed point for this first return map. Accordingly, the creation of different bifurcation structures in a neighborhood of $\mathcal{B}$ is closely related to the problem of a *break up in continuity* at an attracting fixed point.

The question arises how to identify the structures originating from such organizing centers. For a generic codimension-2 BCB point the answer depends on the properties of the cycles which undergo the BCBs. In this paper, we consider the case in which two *stable* cycles of any periods undergo BCBs. We show that *period adding* and *period incrementing* bifurcation structures may issue from the intersection point of the associated bifurcation curves. By period adding bifurcation structure we mean the one in which the periodicity regions of attracting cycles are ordered in the parameter space according to the Farey summation rule [Hardy & Wright, 1960; Apostol, 1990] applied to the rotation numbers of the cycles [Leonov, 1959; Keener, 1980; Homburg, 1996; Gardini *et al.*, 2010; Avrutin *et al.*, 2010]. The period incrementing bifurcation structure represents a sequence of partially pairwise overlapping periodicity regions of attracting cycles with periods which are increased by a constant value in each step [Homburg, 1996; Avrutin & Schanz, 2006; Gardini & Tramontana, 2010; Avrutin *et al.*, 2011; Gardini *et al.*, 2012]. This problem is related to the gluing bifurcations in flows in the case of one-loop homoclinic orbits, as considered by many authors [Gambaudo *et al.*, 1988; Ghrist & Holmes, 1994; Ghrist, 2000].

Our object is to identify which bifurcation structure issues from a codimension-2 BCB point. We construct the *first return map* in a neighborhood of the border point, which is a piecewise smooth map with two contracting branches defined on the left and on the right sides of the border point by suitable compositions of the functions of the original map. Depending on whether these contracting branches are increasing or decreasing, we describe the behavior of the original map in the neighborhood of the codimension-2 BCB point. This is done by proving three separate theorems which consider a codimension-2 BCB point associated with two fixed points colliding on opposite sides of the border point, set to $x = 0$. The theorems differ depending on the local monotonicity of the two functions in a neighborhood of the border point. The assumptions are given mainly on qualitative properties and the proofs are new, depending on topological properties instead of more analytical ones which have recently been published, among which it is worth mentioning [Labarca & Moreira, 2001, 2006; Golmakani & Homburg, 2011; Labarca & Moreira, 2010; Winckler, 2011; Labarca & Vásquez, 2012].

The 1D piecewise smooth maps with one discontinuity point considered here are not only challenging from the theoretical point of view, but also provide an adequate description of the possible dynamics for several one- and higher-dimensional applied models. For example, as recalled above, it is known that the essential dynamics for a class of three-dimensional Lorenz-like flows can be investigated by using a 1D piecewise smooth map. This subject, originated from Lorenz's work [Lorenz, 1963], and since then studied by many researchers. A list of important contributions, although not complete, includes [Guckenheimer & Williams, 1979; Sparrow, 1982; Birman & Williams, 1983; Turaev & Shil'nikov, 1987 (Russian version 1986); Lyubimov *et al.*, 1989; Homburg, 1993, 1996; Ghrist & Holmes, 1993, 1994; Glendinning, 1988]. Thus, to link our theorems in maps with a wide literature on flows, we provide several examples by using the Lorenz maps, showing that the codimension-two points in the considered parameter plane can be rigorously explained by our results.

This paper is organized as follows. In Sec. 2 we consider a generic piecewise smooth 1D map $f$ with one discontinuity point, also called the border point. We assume that in a parameter plane two BCB curves of two different stable cycles $\mathcal{O}_\varrho$ and $\mathcal{O}_\sigma$ transversely intersect in a codimension-2 BCB point $\mathcal{B}$, and that the cycles $\mathcal{O}_\varrho$ and $\mathcal{O}_\sigma$ exist on one side of the corresponding curves and do not exist on the other side. We construct the first return map $\tilde{f}$ in a neighborhood of the border point which describes

[1]Recall that in 1D continuous piecewise smooth maps such a collision occurs at a *nonsmooth fold bifurcation*, also called a *fold BCB*, in which case the colliding cycles are necessarily complementary to each other, that is, their symbolic sequences differ by only one colliding symbol. Given that the condition of fold BCB is the same for both cycles, it defines just one BCB curve.

the behavior of the map $f$ close to point $\mathcal{B}$ and classify the possible cases for a general 1D discontinuous piecewise smooth map, by Theorems 1–3 presented in Sec. 3. In Sec. 3 we first describe the necessary assumptions and in three different subsections we prove the theorems based on the local monotonicity of the functions. In Sec. 3.1 we prove that if the branches are both locally increasing, point $\mathcal{B}$ represents an organizing center from which an infinite number of disjoint periodicity regions of stable cycles issue, organized in a full period adding structure. If one of the local branches is increasing and the other one decreasing, then point $\mathcal{B}$ represents the issuing point of a period incrementing structure, formed by partially overlapping periodicity regions of one infinite family of stable cycles with increasing periods. Finally, if both the branches are decreasing, then from point $\mathcal{B}$ only one more periodicity region issues, thus, this point does not represent an organizing center. This region overlaps partially with each of the existence regions of colliding cycles and is related with a cycle whose symbolic sequence is the concatenation of the symbolic sequences of the colliding ones. For the sake of brevity we call this structure a *coupling bifurcation structure*. In Sec. 4 we recall the relation between Lorenz-like flows and the associated 1D discontinuous piecewise smooth family of maps. For such maps (see [Sparrow, 1982; Glendinning, 1988; Lyubimov *et al.*, 1989; Homburg, 1996; Zaks, 1993]) a codimension-1 BCB point corresponds to the appearance/disappearance of a limit cycle via a homoclinic orbit; a codimension-2 BCB point represents the simultaneous occurrence of two homoclinic orbits (which are merging, or gluing), associated with two different limit cycles. We show that our theorems can be applied to the codimension-2 BCB points which exist in the associated parameter plane. Section 5 concludes.

## 2. Codimension-2 Border Collision Bifurcations

Consider a family of 1D piecewise smooth maps $f$, depending on at least two parameters $\zeta_1$, $\zeta_2$, and defined on two partitions (i.e. different regions of the state space) by two smooth functions $f_{\mathcal{L}}$ and $f_{\mathcal{R}}$ on opposite sides of a border point.[2] Without loss of generality, the border point can be fixed at $x = 0$:

$$x_{n+1} = f(x_n, (\zeta_1, \zeta_2)) = \begin{cases} f_{\mathcal{L}}(x_n, (\zeta_1, \zeta_2)) & \text{if } x_n < 0 \\ f_{\mathcal{R}}(x_n, (\zeta_1, \zeta_2)) & \text{if } x_n > 0. \end{cases} \quad (1)$$

It is well known that the bifurcation structure in the parameter space of these maps may be quite complicated, including infinitely many periodicity regions related to cycles of different periods. Often these regions originate from some particular points, called organizing centers, the investigation of which represents an efficient way to explain the related bifurcation structures.

In the present paper, we consider organizing centers given by the intersections of two BCB curves of two attracting cycles of map $f$. It is worth noting that an organizing center can be obtained not only by an intersection of two BCB curves. For example, in piecewise linear 1D maps a codimension-2 bifurcation point at which a BCB curve intersects a degenerate flip bifurcation curve may represent an organizing center as well (for some examples, see [Avrutin *et al.*, 2006; Gardini & Tramontana, 2011]). On the other hand, as shown below, not every codimension-2 BCB point represents an organizing center. We are interested in the bifurcation structure originating from the intersection point of two BCB curves in a parameter plane of map (1).

Let $\mathcal{O}_\sigma$ and $\mathcal{O}_\varrho$ be two cycles of map (1), with symbolic sequences[3] $\sigma = \sigma_0\sigma_1\cdots\sigma_{p-1}$ and $\varrho = \varrho_0\varrho_1\cdots\varrho_{q-1}$, respectively, where $\sigma_j, \varrho_k \in \{\mathcal{L}, \mathcal{R}\}$ with $j = 0, \ldots, p-1$ and $k = 0, \ldots, q-1$. Let $\xi_\sigma^{\mathcal{L}}$ denote the BCB curve in the parameter plane $(\zeta_1, \zeta_2)$ related to the attracting cycle $\mathcal{O}_\sigma$ at which the point $x_0^\sigma < 0$ of this cycle closest to $x = 0$ from the *left side* collides with the border point, that is, the periodic point satisfies the equation

$$\tilde{f}_{\mathcal{L}}(x_0^\sigma, (\zeta_1, \zeta_2)) = x_0^\sigma, \quad \text{where}$$
$$\tilde{f}_{\mathcal{L}}(x, (\zeta_1, \zeta_2)) := f_{\sigma_p} \circ \cdots \circ f_{\sigma_0}(x, (\zeta_1, \zeta_2)) \quad \text{with } \sigma_0 = \mathcal{L}. \quad (2)$$

[2]Note that in Eq. (1) we do not specify the value of the function $f$ at $x = 0$, as this value has no relevance for the bifurcation structure of the map.

[3]Here we use the standard notation for a symbolic sequence associated with a cycle of a map defined on two partitions: a point of a cycle located in the left half-axis $x < 0$ is associated with the letter $\mathcal{L}$ and a point located in the right half-axis $x > 0$ with the letter $\mathcal{R}$.

At the moment of the border collision we have $x_0^\sigma = 0$, so that the equation $\tilde{f}_{\mathcal{L}}(0,(\zeta_1,\zeta_2)) = 0$ is satisfied. Accordingly, we define the BCB curve as:

$$\xi_\sigma^{\mathcal{L}} = \{(\zeta_1,\zeta_2) \,|\, \tilde{f}_{\mathcal{L}}(0,(\zeta_1,\zeta_2)) = 0\}. \tag{3}$$

We assume that as the parameters cross this BCB curve, the cycle $\mathcal{O}_\sigma$ appears/disappears. Similarly, let $\xi_\varrho^{\mathcal{R}}$ denote the BCB curve of the attracting cycle $\mathcal{O}_\varrho$ at which the point $x_0^\varrho$ of this cycle closest to $x = 0$ from the *right side* collides with the border point, that is, the periodic point satisfies the equation

$$\tilde{f}_{\mathcal{R}}(x_0^\varrho,(\zeta_1,\zeta_2)) = x_0^\varrho, \quad \text{where}$$
$$\tilde{f}_{\mathcal{R}}(x,(\zeta_1,\zeta_2)) := f_{\varrho_q} \circ \cdots \circ f_{\varrho_0}(x,(\zeta_1,\zeta_2)) \quad \text{with } \varrho_0 = \mathcal{R} \tag{4}$$

and we define the BCB curve as:

$$\xi_\varrho^{\mathcal{R}} = \{(\zeta_1,\zeta_2) \,|\, \tilde{f}_{\mathcal{R}}(0,(\zeta_1,\zeta_2)) = 0\}. \tag{5}$$

Now let us assume that the two BCB curves $\xi_\sigma^{\mathcal{L}}$ and $\xi_\varrho^{\mathcal{R}}$ intersect transversely in a codimension-2 BCB point

$$\mathcal{B}_{\sigma/\varrho} = (\bar{\zeta}_1,\bar{\zeta}_2) \in \xi_\sigma^{\mathcal{L}} \cap \xi_\varrho^{\mathcal{R}} \tag{6}$$

and that at the parameter point $\mathcal{B}_{\sigma/\varrho}$ the colliding cycles are hyperbolic (that is, $|\frac{d}{dx}\tilde{f}_{\mathcal{L}}(x,\mathcal{B}_{\sigma/\varrho})|_{x=0} \neq 1$ and $|\frac{d}{dx}\tilde{f}_{\mathcal{R}}(x,\mathcal{B}_{\sigma/\varrho})|_{x=0} \neq 1$).

From the definition of a BCB it follows that for parameter values $\zeta_1,\zeta_2$ belonging to the curve $\xi_\sigma^{\mathcal{L}}$ we have $\tilde{f}_{\mathcal{L}}(0,\mathcal{B}_{\sigma/\varrho}) = 0$ and for parameter values located at the curve $\xi_\varrho^{\mathcal{R}}$ we have $\tilde{f}_{\mathcal{R}}(0,\mathcal{B}_{\sigma/\varrho}) = 0$. Hence, at the codimension-2 BCB point $\mathcal{B}_{\sigma/\varrho}$ the condition

$$\tilde{f}_{\mathcal{L}}(0,\mathcal{B}_{\sigma/\varrho}) = \tilde{f}_{\mathcal{R}}(0,\mathcal{B}_{\sigma/\varrho}) = 0 \tag{7}$$

is satisfied. Thus, a first return map can be constructed, as stated by the following proposition:

**Proposition 1.** *For parameter values in a neighborhood of a point $\mathcal{B}_{\sigma/\varrho}$ belonging to the intersection of two BCB curves as in (6), the first return map in a neighborhood of the point $x = 0$ of the map $f$ given in (1) is defined as follows*:

$$x_{n+1} = \tilde{f}(x_n,(\zeta_1,\zeta_2)) = \begin{cases} \tilde{f}_{\mathcal{L}}(x_n) = f_{\sigma_p} \circ \cdots \circ f_{\sigma_0}(x_n,(\zeta_1,\zeta_2)) \\ \qquad\qquad \text{if } x_n < 0 \\ \tilde{f}_{\mathcal{R}}(x_n) = f_{\varrho_q} \circ \cdots \circ f_{\varrho_0}(x_n,(\zeta_1,\zeta_2)) \\ \qquad\qquad \text{if } x_n > 0. \end{cases} \tag{8}$$

From condition (7) we have that at the point $\mathcal{B}_{\sigma/\varrho}$ the first return map (8) is continuous in $x = 0$. This map represents an adequate tool in investigating the dynamics of map (1) for parameter values in a neighborhood of point $\mathcal{B}_{\sigma/\varrho}$.

From the way in which the map (8) is constructed, it follows that the points $x_0^\sigma$ and $x_0^\varrho$ of the cycles $\mathcal{O}_\sigma$ and $\mathcal{O}_\varrho$ of the original map (1) correspond to two fixed points of the first return map (8), denoted $\tilde{\mathcal{O}}_{\mathcal{L}}$ and $\tilde{\mathcal{O}}_{\mathcal{R}}$, respectively. Accordingly, for the parameter values located at the BCB curve $\xi_\sigma^{\mathcal{L}}$ at which the point $x_0^\sigma$ collides with $x = 0$, the fixed point $\tilde{\mathcal{O}}_{\mathcal{L}}$ of the first return map undergoes a BCB as well. The same also applies to the fixed point $\tilde{\mathcal{O}}_{\mathcal{R}}$ of the first return map and the parameter values located at the BCB curve $\xi_\varrho^{\mathcal{R}}$.

As the attracting cycles $\mathcal{O}_\sigma$ and $\mathcal{O}_\varrho$ exist on one side of the corresponding BCB curve and do not exist on the other side, the bifurcation structure of map (8) in a neighborhood of point $\mathcal{B}_{\sigma/\varrho}$ in the parameter plane $(\zeta_1,\zeta_2)$ is as shown schematically in Fig. 1. The curves $\xi_\sigma^{\mathcal{L}}$ and $\xi_\varrho^{\mathcal{R}}$ (confining the existence regions $\mathcal{P}_\sigma$ and $\mathcal{P}_\varrho$ of the cycles $\mathcal{O}_\sigma$ and $\mathcal{O}_\varrho$, respectively) divide the parameter space into four quadrants. In one of these quadrants both attracting fixed points $\tilde{\mathcal{O}}_{\mathcal{L}}$ and $\tilde{\mathcal{O}}_{\mathcal{R}}$ exist (the corresponding existence regions are denoted by $\tilde{\mathcal{P}}_{\mathcal{L}}$ and $\tilde{\mathcal{P}}_{\mathcal{R}}$, respectively); in two others only one of them exists;

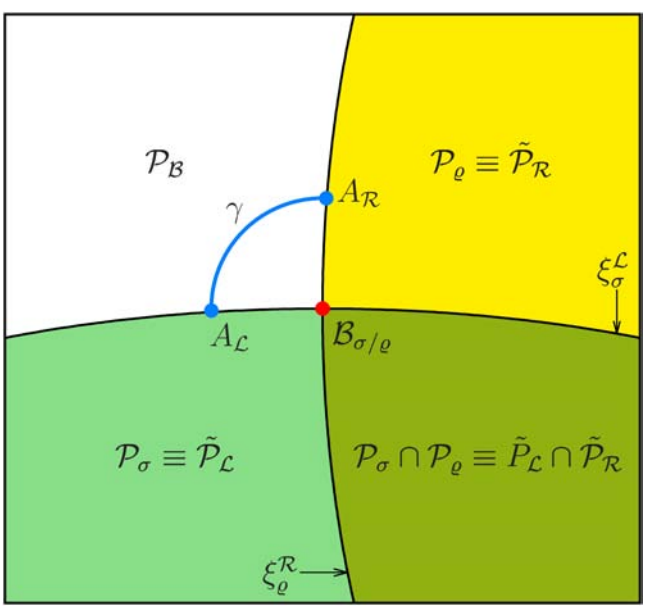


Fig. 1. Schematic structure of the parameter plane of map (1) close to the codimension-2 BCB point $\mathcal{B}_{\sigma/\varrho}$ belonging to the intersection of the BCB curves $\xi_\sigma^{\mathcal{L}}$ and $\xi_\varrho^{\mathcal{R}}$.

and in the remaining quadrant neither $\tilde{\mathcal{O}}_{\mathcal{L}}$ nor $\tilde{\mathcal{O}}_{\mathcal{R}}$ exist. The bifurcation structure of this last quadrant, denoted by $\mathcal{P}_{\mathcal{B}}$, depends mainly on whether the functions $\tilde{f}_{\mathcal{L}}$ and $\tilde{f}_{\mathcal{R}}$ (which are locally contracting) are strictly *increasing* or *decreasing* in a left and right neighborhood of the point $x = 0$, respectively.

A sufficient condition to satisfy these properties comes from the derivatives of the functions $\tilde{f}_{\mathcal{L}}$ and $\tilde{f}_{\mathcal{R}}$ at the origin and at the parameter point $\mathcal{B}_{\sigma/\varrho}$, namely

$$s_{\mathcal{L}} = \frac{d}{dx}\tilde{f}_{\mathcal{L}}(x, \mathcal{B}_{\sigma/\varrho})\bigg|_{x=0}, \qquad s_{\mathcal{R}} = \frac{d}{dx}\tilde{f}_{\mathcal{R}}(x, \mathcal{B}_{\sigma/\varrho})\bigg|_{x=0}. \tag{9}$$

Clearly, $|s_{\mathcal{L}}| < 1$ and $|s_{\mathcal{R}}| < 1$, as the fixed points $\tilde{\mathcal{O}}_{\mathcal{L}}$, $\tilde{\mathcal{O}}_{\mathcal{R}}$ are attracting. If $s_i > 0$ or $s_i < 0$, $i \in \{\mathcal{L}, \mathcal{R}\}$, then a neighborhood of $x = 0$ exists in which $\tilde{f}_i$ is strictly increasing or decreasing, respectively. In the switching case $s_i = 0$ the sign of the lowest order nonzero derivative determines whether locally the branch $\tilde{f}_i$ is strictly increasing or decreasing.

The overall four possible shapes of $\tilde{f}$ for different combinations of $s_{\mathcal{L}}$ and $s_{\mathcal{R}}$ are shown schematically in Fig. 2. It can easily be shown that maps in the configurations 1 and 4 are topologically conjugate and hence have qualitatively the same bifurcation structure.

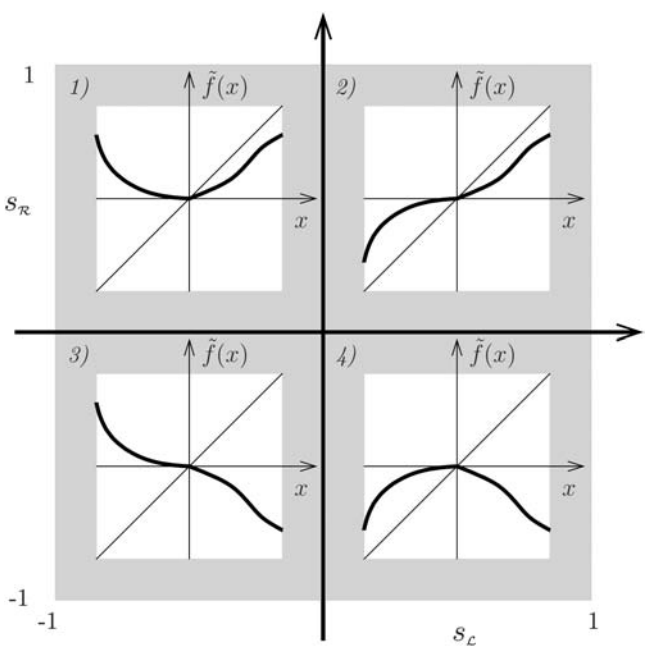


Fig. 2. Schematic representation of possible shapes of the first return map (8) at the codimension-2 point $\mathcal{B}_{\sigma/\varrho}$ associated with BCBs of two stable cycles.

Regarding the monotonicity of the functions $\tilde{f}_{\mathcal{L}}$, $\tilde{f}_{\mathcal{R}}$, if the functions $f_{\mathcal{L}}$ and $f_{\mathcal{R}}$ are increasing in their partitions, then for any pair of cycles $\mathcal{O}_\sigma$, $\mathcal{O}_\varrho$ the branches $\tilde{f}_{\mathcal{L}}$, $\tilde{f}_{\mathcal{R}}$ of the first return map (8) are increasing in the considered neighborhoods as well (since any composition of increasing functions is increasing). Diversely, if at least one of the functions $f_{\mathcal{L}}$, $f_{\mathcal{R}}$ is decreasing, then the branches of the first return map at the parameter point $\mathcal{B}_{\sigma/\varrho}$ may be increasing or decreasing depending on the particular cycles $\mathcal{O}_\sigma$, $\mathcal{O}_\varrho$.

The existence of period adding, period incrementing and coupling bifurcation structures associated with cases A: both increasing functions, B: one increasing function and one decreasing and C: both decreasing functions, is proved, respectively, by applying Theorems 1–3 given in the next section to the first return map $\tilde{f}$ in a neighborhood of point $\mathcal{B}_{\sigma/\varrho}$. Examples of the application of the theorems are given in Sec. 4.

The theorems in Sec. 3 also prove that in a proper neighborhood of a point $\mathcal{B}_{\sigma/\varrho}$ associated with two attracting cycles the bifurcation structure for a generic piecewise smooth map $f$ in Eq. (1) is qualitatively the same as that of piecewise linear maps. A similar connection between generic piecewise smooth maps and piecewise linear maps can also be expected for the case of unstable cycles. Some results regarding the bifurcation structures in piecewise linear maps for generic cases are reported in [Avrutin *et al.*, 2012].

## 3. Continuity Breaking

In this section we consider the case in which the attracting cycles colliding with the border point $x = 0$ are fixed points of a two-parameter family of piecewise smooth maps

$$x_{n+1} = T(x_n; \zeta) = \begin{cases} T_{\mathcal{L}}(x_n; \zeta) & \text{if } x_n < 0 \\ T_{\mathcal{R}}(x_n; \zeta) & \text{if } x_n > 0 \end{cases} \tag{10}$$

where $\zeta = (\zeta_1, \zeta_2)$. We assume that for any $\zeta$ belonging to a suitable region defined below the function $T_{\mathcal{L}}(x; \zeta)$ is smooth for $x \le 0$ and the function $T_{\mathcal{R}}(x; \zeta)$ is smooth for $x \ge 0$. We recall that the definition of map $T$ at the border point $x = 0$ does not affect the bifurcation curves we are interested in, so that at $x = 0$ map $T$ can be defined indifferently as $T_{\mathcal{L}}(0; \zeta)$ or as $T_{\mathcal{R}}(0; \zeta)$.

The sets

$$\xi_{\mathcal{L}} = \{\zeta \,|\, T_{\mathcal{L}}(0;\zeta) = 0\} \quad \text{and} \qquad \xi_{\mathcal{R}} = \{\zeta \,|\, T_{\mathcal{R}}(0;\zeta) = 0\} \tag{11}$$

are related to the collision of fixed points with $x = 0$. That is, if $\zeta \in \xi_{\mathcal{L}}$, then a fixed point of $T_{\mathcal{L}}(x;\zeta)$, say $x^*_{\mathcal{L}}$, is merging with $x = 0$ and similarly if $\zeta \in \xi_{\mathcal{R}}$, then a fixed point of $T_{\mathcal{R}}(x;\zeta)$, say $x^*_{\mathcal{R}}$, is merging with $x = 0$. The following assumptions are considered:

(H1) In the parameter plane $(\zeta_1, \zeta_2)$ a point $\mathcal{B} = (\overline{\zeta}_1, \overline{\zeta}_2) \in \xi_{\mathcal{L}} \cap \xi_{\mathcal{R}}$ exists such that in a neighborhood $W(\mathcal{B})$ of $\mathcal{B}$ the sets $\xi_{\mathcal{L}}$ and $\xi_{\mathcal{R}}$ are two regular curves transversely intersecting in $\mathcal{B}$, and an attracting fixed point $x^*_{\mathcal{L}}$ of $T$ exists on one side of the bifurcation curve $\xi_{\mathcal{L}}$, say for $\{\zeta \,|\, T_{\mathcal{L}}(0;\zeta) < 0\} \subset W(\mathcal{B})$, and does not exist on the other side, for $\{\zeta \,|\, T_{\mathcal{L}}(0;\zeta) > 0\} \subset W(\mathcal{B})$. Similarly for the other bifurcation curve $\xi_{\mathcal{R}}$, an attracting fixed point $x^*_{\mathcal{R}}$ of $T$ exists on one side of the bifurcation curve $\xi_{\mathcal{R}}$, and does not exist on the other side.

(H2) $T_i(x;(\zeta_1,\zeta_2))$ is differentiable with respect to $\zeta_1$ and $\zeta_2$ in $x = 0$, $\zeta = \mathcal{B}$, and $|T'_i(x;\zeta)|_{(x=0;\zeta=\mathcal{B})}| < 1$ for $i = \mathcal{L}, \mathcal{R}$.

It follows from our assumptions on $T_i(x;\zeta)$ in $(0;\mathcal{B})$ that a neighborhood $U(\mathcal{B}) \subset W(\mathcal{B})$ of $\mathcal{B}$ exists such that for any $\zeta \in U(\mathcal{B})$ the two functions $T_{\mathcal{L}}(x;\zeta)$ and $T_{\mathcal{R}}(x;\zeta)$ are contracting in a left and right neighborhood of $x = 0$, respectively, say in $J_{\mathcal{L}}$ and $J_{\mathcal{R}}$. Then let us also assume that

(H3) $T_i(x;\zeta)$ is strictly monotone in $J_i$ for any $\zeta \in U(\mathcal{B})$, $i = \mathcal{L}, \mathcal{R}$.[4]

In the neighborhood $U(\mathcal{B})$ (as shown qualitatively in Fig. 1) the set $\xi_{\mathcal{L}}$ (resp. $\xi_{\mathcal{R}}$) is an arc of the BCB curve associated with the appearance/disappearance of a fixed point $x^*_{\mathcal{L}}$ from the left side (resp. $x^*_{\mathcal{R}}$ from the right side) of the discontinuity, and $\mathcal{B}$ is a codimension-2 bifurcation point. For parameters $\zeta$ in $U(\mathcal{B})$ belonging to the overlapping of the two existence regions, both attracting fixed points exist in map $T$, one in $J_{\mathcal{L}}$ and one in $J_{\mathcal{R}}$, and we can assume (eventually decreasing $U(\mathcal{B})$) that $T_{\mathcal{L}}(0;\zeta)$ converges to $x^*_{\mathcal{L}}$ while $T_{\mathcal{R}}(0;\zeta)$ converges to $x^*_{\mathcal{R}}$.[5] For parameters in the neighborhood $U(\mathcal{B})$ belonging to the two regions adjacent to the overlapping one, map $T$ has only one fixed point in $J_{\mathcal{L}} \cup J_{\mathcal{R}}$, either in $J_{\mathcal{L}}$ or in $J_{\mathcal{R}}$. Meanwhile for parameters in the neighborhood $U(\mathcal{B})$ belonging to the remaining region $\mathcal{P}_{\mathcal{B}}$, the map $T$ has no fixed points in $J_{\mathcal{L}} \cup J_{\mathcal{R}}$. The object of the present section is to describe the bifurcation structure existing in the region $\mathcal{P}_{\mathcal{B}}$. We have assumed monotone functions in $J_i$ for any $\zeta \in U(\mathcal{B})$ and thus the shape of the functions at the bifurcation moment, when the parameters are on the bifurcation curves bounding region $\mathcal{P}_{\mathcal{B}}$ is known. What we consider afterwards is any arc (or segment of a straight line) $\gamma$ connecting two points on these curves, say $A_{\mathcal{R}} \in \xi_{\mathcal{R}}$ and $A_{\mathcal{L}} \in \xi_{\mathcal{L}}$ in the region $\mathcal{P}_{\mathcal{B}}$ in $U(\mathcal{B})$ as qualitatively shown in Fig. 1. The offsets $T_{\mathcal{R}}(0,\zeta)$ and $T_{\mathcal{L}}(0,\zeta)$ in the point $A_{\mathcal{L}}$ satisfy $T_{\mathcal{R}}(0,\zeta) < T_{\mathcal{L}}(0,\zeta) = 0$, while in point $A_{\mathcal{R}}$ it is $0 = T_{\mathcal{R}}(0,\zeta) < T_{\mathcal{L}}(0,\zeta)$. Then we assume that

(H4) As a parameter point $\zeta$ moves from $A_{\mathcal{L}} \in \xi_{\mathcal{L}}$ to $A_{\mathcal{R}} \in \xi_{\mathcal{R}}$ along any segment $\gamma$ in $\mathcal{P}_{\mathcal{B}}$ where $T$ has no fixed points, the offsets $T_{\mathcal{L}}(0;\zeta)$ and $T_{\mathcal{R}}(0;\zeta)$ are increasing.

Notice that at the parameter point $\mathcal{B}$ the map is continuous in $x = 0$ as $T_{\mathcal{L}}(0;\mathcal{B}) = T_{\mathcal{R}}(0;\mathcal{B}) = 0$ which is a fixed point, so that Theorems 1–3 proved in this section also describe *the results of a continuity breaking in a locally attracting fixed point*, under the assumption of locally monotone functions on both sides of the fixed point $x = 0$.

In the following, to simplify the notation, we shall omit (when not explicitly needed) the dependence of $T$ on the parameter point $\zeta$, writing simply $T(x) = T_{\mathcal{L}}(x)$ for $x < 0$ and $T(x) = T_{\mathcal{R}}(x)$ for $x > 0$.

### 3.1. *Period adding structure*

The proof of Theorem 1 (given in this subsection) follows reasoning similar to that in [Homburg, 1996]

[4]We note that by replacing this condition with the assumption $T'_i(x;b)|_{(x=0;b=\mathcal{B})} \neq 0$ for $i = \mathcal{L}, \mathcal{R}$ we have strict monotonicity, but we prefer to use less restrictive assumptions, which allow us also to deal with the condition $T'_i(x;\zeta)|_{(x=0;\zeta=\mathcal{B})} = 0$ for $i = \mathcal{L}$ and/or $\mathcal{R}$.

[5]As the values at the discontinuity point (or offsets, or critical points) converge on the attracting fixed points, the discontinuity point $x = 0$ and its preimages belong to the frontier of the related basins of attraction for $T$.

(Sec. 3.2). Moreover, we make use of the complexity levels introduced by Leonov [1959], as in [Gardini *et al.*, 2010; Tramontana *et al.*, 2012] for piecewise linear maps.

**Theorem 1.** *Let $T$ in Eq. (10) satisfy assumptions (H1)–(H4) given above. If for any $\zeta \in U(\mathcal{B})$ the functions $T_{\mathcal{L}}(x;\zeta)$ and $T_{\mathcal{R}}(x;\zeta)$ are strictly increasing in the intervals $J_{\mathcal{L}}$ and $J_{\mathcal{R}}$, respectively, then $\mathcal{B}$ is an organizing center of a full period adding structure.*

*Proof.* Let us consider the region $\mathcal{P}_{\mathcal{B}}$ in $U(\mathcal{B})$ bounded by the BCB curves $\xi_{\mathcal{L}}$ and $\xi_{\mathcal{R}}$, associated with no fixed points of $T$ in the no-escape interval,[6] where we can assume (eventually decreasing $U(\mathcal{B})$) $[0, T_{\mathcal{L}}(0)] \subset J_{\mathcal{R}}$ and $[T_{\mathcal{R}}(0), 0] \subset J_{\mathcal{L}}$ $I = [T_{\mathcal{R}}(0), T_{\mathcal{L}}(0)]$. Then for parameters belonging to the interior of $\mathcal{P}_{\mathcal{B}}$ the map $T$ is a gap-map in $I$, with the gap $Z_0 = (T_{\mathcal{R}} \circ T_{\mathcal{L}}(0), T_{\mathcal{L}} \circ T_{\mathcal{R}}(0))$.

When the parameters belong to curve $\xi_{\mathcal{L}}$ on the boundary of $\mathcal{P}_{\mathcal{B}}$ [let $A_{\mathcal{L}}$ be such a point, see Fig. 3(e)], map $T$ has the fixed point $x = 0$. This fixed point attracts all initial conditions from the interval $I = [T_{\mathcal{R}}(0), 0]$ (whose trajectories have the symbolic sequence $\mathcal{L}^{\infty}$), and all initial conditions from the interval $(0, T_{\mathcal{R}}^{-1}(0))$ (whose trajectories have the symbolic sequence $\mathcal{R}\mathcal{L}^{\infty}$), see Fig. 3(f). Similarly, when the parameters belong to curve $\xi_{\mathcal{R}}$ on the boundary of $\mathcal{P}_{\mathcal{B}}$ [let $A_{\mathcal{R}}$ be such a point, see Fig. 3(e)], the fixed point $x = 0$ of the map $T$ attracts all the points of $I = [0, T_{\mathcal{L}}(0)]$ (having

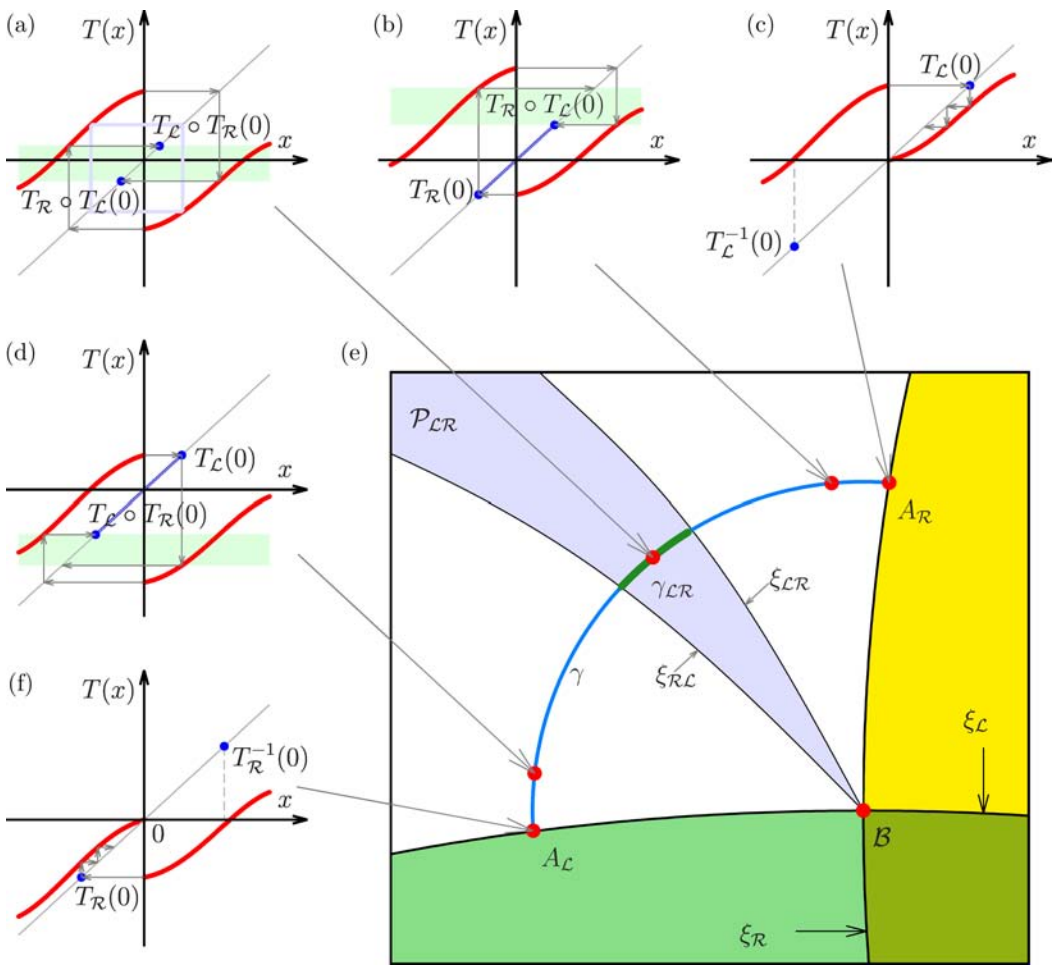


Fig. 3. Schematic structure of the parameter plane of map $T$ in the neighborhood $U(\mathcal{B})$ of point $\mathcal{B}$ when $T$ is defined by two increasing functions.

[6]A no-escape or a trapping interval is an interval which is mapped into itself, i.e. an interval from which the trajectories cannot escape.

trajectories with the symbolic sequence $\mathcal{R}^\infty$), and the points from the interval $(T_{\mathcal{L}}^{-1}(0), 0)$, (having trajectories with the symbolic sequence $\mathcal{LR}^\infty$) see Fig. 3(c).

Consider an arc $\gamma$ in the region $\mathcal{P}_{\mathcal{B}}$ connecting $A_{\mathcal{R}}$ with $A_{\mathcal{L}}$ [see Fig. 3(e)]. When a parameter point belongs to the arc $\gamma$ then the absorbing interval must include the discontinuity point and it can be written as

$$\begin{aligned} I &= [T_{\mathcal{R}}(0), T_{\mathcal{L}}(0)] \\ &= [T_{\mathcal{R}}(0), T_{\mathcal{R}} \circ T_{\mathcal{L}}(0)] \cup Z_0 \\ &\quad \cup [T_{\mathcal{L}} \circ T_{\mathcal{R}}(0), T_{\mathcal{L}}(0)]. \end{aligned} \tag{12}$$

When the parameter point is close to point $A_{\mathcal{R}}$ then the discontinuity point $x = 0$ must belong to the interval $[T_{\mathcal{R}}(0), T_{\mathcal{R}} \circ T_{\mathcal{L}}(0)]$ [see Fig. 3(b)], while when the parameter point is close to $A_{\mathcal{L}}$, the discontinuity point $x = 0$ must belong to the interval $[T_{\mathcal{L}} \circ T_{\mathcal{R}}(0), T_{\mathcal{L}}(0)]$ [see Fig. 3(d)]. It follows that, starting from one end point of $\gamma$, say $A_{\mathcal{R}}$, and moving the parameters along the arc $\gamma$, before reaching point $A_{\mathcal{L}}$ there is a segment of $\gamma$ for which $x = 0$ belongs to $Z_0$ [see Fig. 3(a)]. A gap-map with the discontinuity point in the gap $Z_0$ necessarily has at least one cycle of period 2, with the symbolic sequence $\mathcal{LR}$. In fact, the map $T^2(x) = T_{\mathcal{L}} \circ T_{\mathcal{R}}(x)$ is continuous and increasing in $[0, T_{\mathcal{L}}(0)]$ and $T^2([0, T_{\mathcal{L}}(0)]) \subset [0, T_{\mathcal{L}}(0)]$ (as $T^2(0) > 0$ and $T^2(T_{\mathcal{L}}(0)) < T_{\mathcal{L}}(0)$). Thus, at least one attracting 2-cycle of the map $T$ exists, which under our assumptions ($T^2$ is a contraction on the left and right neighborhoods of $x = 0$ in $I$) is unique and globally attracting in $I$. As the parameter point moves from $A_{\mathcal{R}}$ to $A_{\mathcal{L}}$, the offsets decrease (by assumption (H4)), and it follows from (12) that the first BCB curve which is met, say $\xi_{\mathcal{LR}}$, is given by $T_{\mathcal{R}} \circ T_{\mathcal{L}}(0) = 0$ at which the 2-cycle is colliding with the discontinuity point $x = 0$ from the left side, while on the second curve, say $\xi_{\mathcal{RL}}$, given by $T_{\mathcal{L}} \circ T_{\mathcal{R}}(0) = 0$, the 2-cycle is colliding with $x = 0$ from the right side. Note that the symbolic sequence $\mathcal{LR}$ of the 2-cycle is just a concatenation of the starting symbols $\mathcal{L}$ and $\mathcal{R}$ related to the colliding fixed points.

Summarizing, we have shown that [see Fig. 3(e)]

- in the arc $\gamma$ there exists a segment, say $\gamma_{\mathcal{LR}}$, associated with a 2-cycle with symbolic sequence $\mathcal{LR}$;
- the BCBs occurring at the boundaries of the arc $\gamma_{\mathcal{LR}}$ are given by implicit equations:

$$\xi_{\mathcal{RL}} = \{T_{\mathcal{L}} \circ T_{\mathcal{R}}(0) = 0\} \tag{13a}$$

$$\xi_{\mathcal{LR}} = \{T_{\mathcal{R}} \circ T_{\mathcal{L}}(0) = 0\} \tag{13b}$$

- segment $\gamma_{\mathcal{LR}}$ is an internal subset of $\gamma$, and moving from $A_{\mathcal{R}}$ to $A_{\mathcal{L}}$ the order of the bifurcation curves is $\xi_{\mathcal{R}}$, $\xi_{\mathcal{LR}}$, $\xi_{\mathcal{RL}}$, $\xi_{\mathcal{L}}$.

Clearly point $\mathcal{B}$ satisfies both equations in (13) (as $T_{\mathcal{L}}(0) = 0$ and $T_{\mathcal{R}}(0) = 0$ in $\mathcal{B}$), so that these equations define curves in the parameter plane issuing from $\mathcal{B}$. Hence, instead of an arc $\gamma_{\mathcal{LR}}$ we can consider a periodicity region $\mathcal{P}_{\mathcal{LR}}$ issuing from the point $\mathcal{B}$ bounded by $\xi_{\mathcal{RL}}$ and $\xi_{\mathcal{LR}}$ [see Fig. 3(e)].

The steps performed above, leading to the 2-cycle, can now be repeated considering the region bounded by the bifurcation curves $\xi_{\mathcal{LR}}$ and $\xi_{\mathcal{R}}$ on one side of the periodicity region $\mathcal{P}_{\mathcal{LR}}$, and the region bounded by $\xi_{\mathcal{RL}}$ and $\xi_{\mathcal{L}}$ on the other side. Let us consider the first region (as for the second one the reasoning is the same, with the symbols $\mathcal{L}$ and $\mathcal{R}$ exchanged).

So let us consider the portion on the arc $\gamma$ between the curves $\xi_{\mathcal{LR}}$ and $\xi_{\mathcal{R}}$ [see Fig. 3(e)]. We can argue as before with map $F(x)$ defined as $F_{\mathcal{L}} = T_{\mathcal{R}} \circ T_{\mathcal{L}}(x)$ in a left neighborhood of $x = 0$, satisfying $F_{\mathcal{L}}(0) = 0$ on the point belonging to $\xi_{\mathcal{LR}}$, and $F_{\mathcal{R}} = T_{\mathcal{R}}(x)$ in a right neighborhood of $x = 0$, satisfying $F_{\mathcal{R}}(0) = 0$ on the point $A_{\mathcal{R}}$ (on $\xi_{\mathcal{R}}$). Both branches $F_{\mathcal{L}}$ and $F_{\mathcal{R}}$ are increasing and contracting, and when the parameters are moved from $\xi_{\mathcal{R}}$ to $\xi_{\mathcal{LR}}$ the offset $F_{\mathcal{L}}(0) = T_{\mathcal{R}} \circ T_{\mathcal{L}}(0)$ decreases monotonously from a positive value to zero, as explained above. Thus map $F$ is in the same configuration as map $T$ (with $F_{\mathcal{L}}$ and $F_{\mathcal{R}}$ in place of $T_{\mathcal{L}}$ and $T_{\mathcal{R}}$). Therefore, between $\xi_{\mathcal{LR}}$ and $\xi_{\mathcal{R}}$ an arc associated with a 2-cycle of $F$ in the interval $[F_{\mathcal{R}}(0), F_{\mathcal{L}}(0)] = [T_{\mathcal{R}}(0), T_{\mathcal{R}} \circ T_{\mathcal{L}}(0)]$ must exist. The related cycle has the symbolic sequence $\mathcal{LR}$ for $F$ and $\mathcal{LR}^2$ for $T$. The BCB curves of this cycle are given by the following implicit equations:

$$\xi_{\mathcal{R}(\mathcal{LR})} = \{F_{\mathcal{L}} \circ F_{\mathcal{R}}(0) = T_{\mathcal{R}} \circ T_{\mathcal{L}} \circ T_{\mathcal{R}}(0) = 0\}, \tag{14a}$$

$$\xi_{(\mathcal{LR})\mathcal{R}} = \{F_{\mathcal{R}} \circ F_{\mathcal{L}}(0) = T_{\mathcal{R}} \circ T_{\mathcal{R}} \circ T_{\mathcal{L}}(0) = 0\}. \tag{14b}$$

These BCB curves bound the periodicity region issuing from $\mathcal{B}$, related to the 3-cycle of $T$ with the symbolic sequence $\mathcal{LR}^2$.

Similarly, it is possible to show the existence of periodicity regions of maximal cycles having symbolic sequences $\mathcal{LR}^{n_1}$ for any $n_1$. The BCB curves bounding these regions are given by implicit equations as follows:

$$\xi_{\mathcal{RLR}^{n_1-1}} = \{T_{\mathcal{R}}^{n_1-1} \circ T_{\mathcal{L}} \circ T_{\mathcal{R}}(0) = 0\} \quad (15a)$$

$$\xi_{\mathcal{LR}^{n_1}} = \{T_{\mathcal{R}}^{n_1} \circ T_{\mathcal{L}}(0) = 0\}. \quad (15b)$$

The related periodicity regions accumulate on the bifurcation curve $\xi_{\mathcal{R}}$. In fact, from our assumptions on $T_{\mathcal{R}}(x)$ it follows that $T_{\mathcal{R}}^{n}(x_0) \to 0_+$ as $n \to \infty$ for any $x_0 \in [0, T_{\mathcal{L}}(0)]$. Thus, in the limit, $T_{\mathcal{R}}(0) = 0$ holds, which is the equation of the BCB curve $\xi_{\mathcal{R}}$.

As already noted, all the periodicity regions of maximal cycles with the symbolic sequence $\mathcal{RL}^{n_1}$ for any $n_1$ must also exist, with BCB curves given by implicit equations as follows:

$$\xi_{\mathcal{LRL}^{n_1-1}} = \{T_{\mathcal{L}}^{n_1-1} \circ T_{\mathcal{R}} \circ T_{\mathcal{L}}(0) = 0\} \quad (16a)$$

$$\xi_{\mathcal{RL}^{n_1}} = \{T_{\mathcal{L}}^{n_1} \circ T_{\mathcal{R}}(0) = 0\} \quad (16b)$$

which accumulate on the bifurcation curve $\xi_{\mathcal{L}}$ (as follows from our assumptions on $T_{\mathcal{L}}(x)$ and reasoning as above).

The regions related to maximal cycles constitute the periodicity regions of the *first complexity level*. They all exist, issue from point $\mathcal{B}$, and, as we have seen above, are disjoint. Now, considering the space between any two consecutive regions of the first complexity level (i.e. without any other periodicity region of the first complexity level in between), say the region bounded by $\xi_{\mathcal{LR}^{n_1}}$ and $\xi_{\mathcal{RLR}^{n_1}}$ [whose equations are given in (15)], we have that these two BCB curves correspond to collisions of cycles on opposite sides of $x = 0$. Namely, curve $\xi_{\mathcal{LR}^{n_1}}$ corresponds to a collision of the periodic point $x_0$ of the cycle with the symbolic sequence $\mathcal{LR}^{n_1}$ from the left side of $x = 0$ (that is, the colliding point satisfies $T_{\mathcal{R}}^{n_1} \circ T_{\mathcal{L}}(x_0) = x_0$). Meanwhile, curve $\xi_{\mathcal{RLR}^{n_1}}$ corresponds to a collision of the periodic point $x_0$ of the cycle with the symbolic sequence $\mathcal{RLR}^{n_1}$ on the right side of $x = 0$ (that is, the colliding point satisfies $T_{\mathcal{R}}^{n_1} \circ T_{\mathcal{L}} \circ T_{\mathcal{R}}(x_0) = x_0$). Thus, for the segment of $\gamma$ between $\xi_{\mathcal{LR}^{n_1}}$ and $\xi_{\mathcal{RLR}^{n_1}}$ we can repeat the same arguments as above for any $n_1$, and obtain two infinite families of periodicity regions with the two starting curves $\xi_{\mathcal{LR}^{n_1}}$ and $\xi_{\mathcal{RLR}^{n_1}}$ as limit sets. One family of periodicity regions is related to cycles with the symbolic sequence $\mathcal{LR}^{n_1}(\mathcal{RLR}^{n_1})^{n_2}$, for any $n_2$, and these regions are bounded by the BCB curves which satisfy the following implicit equations:

$$\xi_{(\mathcal{RLR}^{n_1})\mathcal{LR}^{n_1}(\mathcal{RLR}^{n_1})^{n_2-1}} = \{(T_{\mathcal{R}}^{n_1} \circ T_{\mathcal{L}} \circ T_{\mathcal{R}})^{n_2-1} \circ (T_{\mathcal{R}}^{n_1} \circ T_{\mathcal{L}}) \circ (T_{\mathcal{R}}^{n_1} \circ T_{\mathcal{L}} \circ T_{\mathcal{R}})(0) = 0\} \quad (17a)$$

$$\xi_{\mathcal{LR}^{n_1}(\mathcal{RLR}^{n_1})^{n_2}} = \{(T_{\mathcal{R}}^{n_1} \circ T_{\mathcal{L}} \circ T_{\mathcal{R}})^{n_2} \circ T_{\mathcal{R}}^{n_1} \circ T_{\mathcal{L}}(0) = 0\}. \quad (17b)$$

These curves issue from point $\mathcal{B}$ and accumulate on the curve $\xi_{\mathcal{RLR}^{n_1}}$. The second family of periodicity regions is related to cycles having the symbolic sequence $\mathcal{RLR}^{n_1}(\mathcal{LR}^{n_1})^{n_2}$. The corresponding BCB curves are given by

$$\xi_{\mathcal{RLR}^{n_1}(\mathcal{LR}^{n_1})^{n_2}} = \{(T_{\mathcal{R}}^{n_1} \circ T_{\mathcal{L}})^{n_2} \circ (T_{\mathcal{R}}^{n_1} \circ T_{\mathcal{L}} \circ T_{\mathcal{R}})(0) = 0\} \quad (18a)$$

$$\xi_{(\mathcal{LR}^{n_1})\mathcal{RLR}^{n_1}(\mathcal{LR}^{n_1})^{n_2-1}} = \{(T_{\mathcal{R}}^{n_1} \circ T_{\mathcal{L}})^{n_2-1} \circ (T_{\mathcal{R}}^{n_1} \circ T_{\mathcal{L}} \circ T_{\mathcal{R}}) \circ (T_{\mathcal{R}}^{n_1} \circ T_{\mathcal{L}})(0) = 0\} \quad (18b)$$

and accumulate on $\xi_{\mathcal{LR}^{n_1}}$.

The same arguments can be repeated with respect to the other side of the 2-periodicity region, that is, in the region bounded by $\xi_{\mathcal{L}}$ and $\xi_{\mathcal{RL}}$. The regions of the first complexity level associated with cycles with symbolic sequences $\mathcal{RL}^{n_1}$ must exist, whose BCB curves are as given in (16). Between any pair of regions related to the symbolic sequences $\mathcal{RL}^{n_1}$ and $\mathcal{LRL}^{n_1}$, two infinite families of periodicity regions of cycles of second complexity level must exist with the symbolic sequences $\mathcal{RL}^{n_1}(\mathcal{LRL}^{n_1})^{n_2}$ and $\mathcal{LRL}^{n_1}(\mathcal{RL}^{n_1})^{n_2}$, for any $n_2 > 0$. The BCB curves of these cycles are given in (17a)–(18b) with the symbols $\mathcal{L}$ and $\mathcal{R}$ interchanged.

As all these regions, issuing from $\mathcal{B}$, intersect the arc $\gamma$ in disjoint segments, the process can continue *ad infinitum*. Between any two consecutive regions of the second complexity level (that is, without other regions of the second complexity level between them) there exist periodicity regions of the *third complexity level* (two infinite families accumulating on the starting BCB curves).

In general, between any two consecutive regions of the same complexity level $k$ there exist two

families of regions of complexity level $k+1$. As already stated, when the parameters belong to any periodicity region, the related gap map $T$ has a unique attracting cycle with a rational rotation number. From the process described above it follows that the rotation numbers of the cycles of complexity level $k+1$ are obtained from the rotation numbers of the cycles of complexity level $k$ applying the Farey summation rule (see [Gardini *et al.*, 2010] for details). The periodicity regions of all complexity levels densely fill region $\mathcal{P}_{\mathcal{B}}$, except for particular curves which are related to irrational rotation numbers (the related attracting set of $T$ is a Cantor set attractor) (see [Keener, 1980]).

We note that the reasoning used above can be applied to the region between any pair of BCB curves, associated with the collision of different cycles on opposite sides of $x=0$, having any kind of symbolic sequences (one starting with $\mathcal{L}$ and the other one with $\mathcal{R}$). The existence of a cycle with a symbolic sequence obtained by the concatenation of the sequences of the colliding cycles is in any case true, but the period of such a cycle is prime only if the starting cycles have rotation numbers which are Farey neighbors.[7] ■

Let us now consider two cycles $\mathcal{O}_\sigma$ and $\mathcal{O}_\varrho$ of map (1), and let $\mathcal{B}_{\sigma/\varrho}$ be a point at which two BCB curves $\xi_\sigma^{\mathcal{L}}$ and $\xi_\varrho^{\mathcal{R}}$ intersect transversely, satisfying the assumptions of Theorem 1. By Theorem 1 applied to the first return map $\tilde{f}$ given by Eq. (8) we have that the point $\mathcal{B}_{\sigma/\varrho}$ is an organizing center of a full period adding structure. The bifurcation structure in the parameter plane around the point $\mathcal{B}_{\sigma/\varrho}$ is shown schematically in Fig. 4.

As shown above, the periodicity regions forming the period adding structure are ordered according to the Farey summation rule applied to the rotation numbers of the related cycles. Namely, if the rotation numbers $\rho_1 = \frac{p_1}{q_1}$ and $\rho_2 = \frac{p_2}{q_2}$ are Farey neighbors, then between the periodicity regions of the cycles with the rotation numbers $\rho_1$ and $\rho_2$ there exists a periodicity region of a cycle with the rotation number $\rho_1 \oplus \rho_2 = \frac{p_1+p_2}{q_1+q_2}$. In this case, if the cycle with the rotation number $\rho_1$ has the symbolic sequence $\sigma$ and the one with the rotation number $\rho_2$ has the symbolic sequence $\varrho$, then the cycle with the rotation number $\rho_1 \oplus \rho_2$ has the symbolic sequence $\sigma\varrho$ obtained by the concatenation of the symbolic sequences $\sigma$ and $\varrho$.[8] Accordingly, for the first return map (8) we can specify the families of attracting cycles whose existence regions issue from the point $\mathcal{B}_{\sigma/\varrho}$. In particular, between the existence regions of the fixed points $\tilde{\mathcal{O}}_{\mathcal{L}}$ and $\tilde{\mathcal{O}}_{\mathcal{R}}$ there are two families of the existence regions of attracting cycles

$$\{\tilde{\mathcal{O}}_{\mathcal{R}\mathcal{L}^{n_1}} \,|\, n_1 > 0\}, \quad \{\tilde{\mathcal{O}}_{\mathcal{L}\mathcal{R}^{n_1}} \,|\, n_1 > 0\}. \tag{19}$$

These cycles (frequently called maximal, or principal, or basic) are referred to as cycles with the *complexity level one* [Leonov, 1959; Gardini *et al.*, 2010; Avrutin *et al.*, 2010].

For each $n_1$ the existence region $\tilde{\mathcal{P}}_{\mathcal{R}\mathcal{L}^{n_1}}$ of cycle $\tilde{\mathcal{O}}_{\mathcal{R}\mathcal{L}^{n_1}}$ is bounded by the BCB curves given by

$$\xi_{\mathcal{L}\mathcal{R}\mathcal{L}^{n_1-1}} = \{\tilde{f}_{\mathcal{L}}^{n_1-1} \circ \tilde{f}_{\mathcal{R}} \circ \tilde{f}_{\mathcal{L}}(0) = 0\} \tag{20a}$$

$$\xi_{\mathcal{R}\mathcal{L}^{n_1}} = \{\tilde{f}_{\mathcal{L}}^{n_1} \circ \tilde{f}_{\mathcal{R}}(0) = 0\} \tag{20b}$$

whereby the definition of the functions $\tilde{f}_{\mathcal{L}}$, $\tilde{f}_{\mathcal{R}}$ depends on the particular cycles $\mathcal{O}_\sigma$, $\mathcal{O}_\varrho$ as given by Eq. (8) (see examples in Sec. 4). Similarly, the existence region $\tilde{\mathcal{P}}_{\mathcal{L}\mathcal{R}^{n_1}}$ of the cycle $\tilde{\mathcal{O}}_{\mathcal{L}\mathcal{R}^{n_1}}$ is bounded by the BCB curves

$$\xi_{\mathcal{L}\mathcal{R}^{n_1}} = \{\tilde{f}_{\mathcal{R}}^{n_1} \circ \tilde{f}_{\mathcal{L}}(0) = 0\} \tag{21a}$$

$$\xi_{\mathcal{R}\mathcal{L}\mathcal{R}^{n_1-1}} = \{\tilde{f}_{\mathcal{R}}^{n_1-1} \circ \tilde{f}_{\mathcal{L}} \circ \tilde{f}_{\mathcal{R}}(0) = 0\}. \tag{21b}$$

Note that if the functions $f_{\mathcal{L}}$, $f_{\mathcal{R}}$ are linear,[9] and hence the functions $\tilde{f}_{\mathcal{L}}$, $\tilde{f}_{\mathcal{R}}$ are linear as well, then for any $n_1$ the implicit equations of the BCB curves given by (20) and (21) can be solved explicitly with respect to the offsets of the functions $f_{\mathcal{L}}$, $f_{\mathcal{R}}$ [Leonov, 1959; Gardini *et al.*, 2010; Avrutin *et al.*, 2010]. In general this is not the case.

All the related regions are disjoint and in the space between two consecutive existence regions $\tilde{\mathcal{P}}_{\mathcal{R}\mathcal{L}^{n_1}}$ and $\tilde{\mathcal{P}}_{\mathcal{R}\mathcal{L}^{n_1+1}}$ of the cycles $\tilde{\mathcal{O}}_{\mathcal{R}\mathcal{L}^{n_1}}$ and $\tilde{\mathcal{O}}_{\mathcal{R}\mathcal{L}^{n_1+1}}$ for each $n_1$ there are two families of

[7]Recall that two irreducible fractions $\rho_1 = \frac{p_1}{q_1}$ and $\rho_2 = \frac{p_2}{q_2}$ are called Farey neighbors iff $|p_2 q_1 - p_1 q_2| = 1$.

[8]Recall that symbolic sequences associated with cycles are shift-invariant. However, when dealing with the concatenation of sequences and also with the specification of the BCB curves, they must be cyclically shifted in such a way that the point of the associated cycle which collides with the border point corresponds to the first letter $\sigma_0$ and $\varrho_0$, respectively, as in Eqs. (2) and (4).

[9]Here "linear" is used in the wider meaning of "affine".

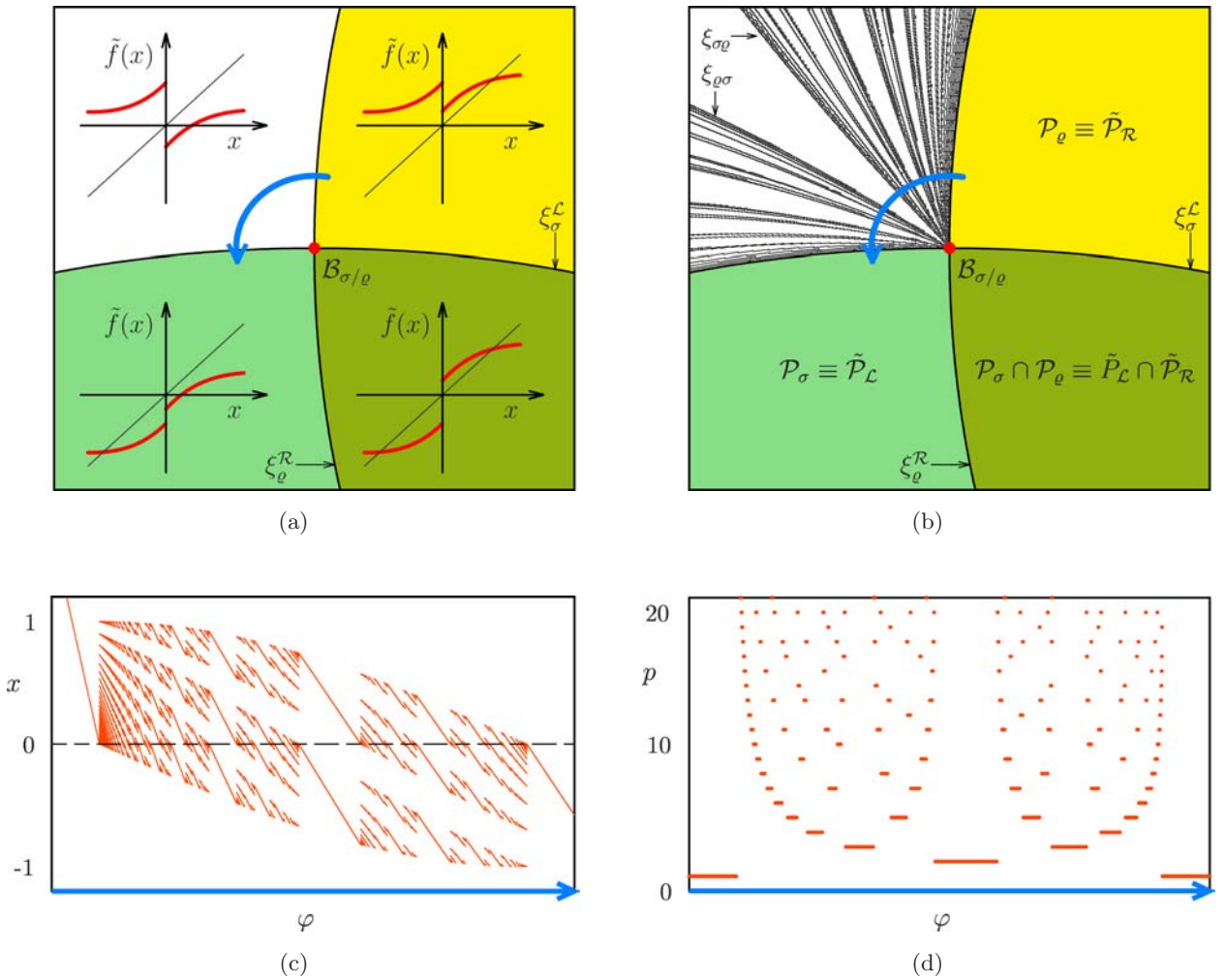


Fig. 4. In (a) the shapes of the first return map (8) in the increasing–increasing configuration, and (b) the bifurcation structures close to the intersection point $\mathcal{B}_{\sigma/\varrho}$ of the border collision bifurcation curves $\tilde{\xi}_{\mathcal{L}}$ and $\tilde{\xi}_{\mathcal{R}}$ are shown schematically. (c) and (d) show the associated bifurcation and period ($p$) diagrams, respectively, under variation of the angle $\varphi$ along the arc marked blue in (a) and (b).

regions associated with the cycles of *complexity level two*:

$$\begin{aligned}&\{\tilde{\mathcal{O}}_{\mathcal{R}\mathcal{L}^{n_1}(\mathcal{L}\mathcal{R}\mathcal{L}^{n_1})^{n_2}} \,|\, n_i > 0, i = 1, 2\},\\ &\{\tilde{\mathcal{O}}_{\mathcal{L}\mathcal{R}\mathcal{L}^{n_1}(\mathcal{R}\mathcal{L}^{n_1})^{n_2}} \,|\, n_i > 0, i = 1, 2\}.\end{aligned} \tag{22}$$

The BCB curves for the first of these families are given by

$$\begin{aligned}&\xi_{\mathcal{L}\mathcal{R}\mathcal{L}^{n_1}\mathcal{R}\mathcal{L}^{n_1}(\mathcal{L}\mathcal{R}\mathcal{L}^{n_1})^{n_2-1}}\\ &\quad = \{(\tilde{f}_{\mathcal{L}}^{n_1} \circ \tilde{f}_{\mathcal{R}} \circ \tilde{f}_{\mathcal{L}})^{n_2-1}\\ &\qquad \circ \tilde{f}_{\mathcal{L}}^{n_1} \circ \tilde{f}_{\mathcal{R}} \circ \tilde{f}_{\mathcal{L}}^{n_1} \circ \tilde{f}_{\mathcal{R}} \circ \tilde{f}_{\mathcal{L}}(0) = 0\}\end{aligned} \tag{23a}$$

$$\begin{aligned}&\xi_{\mathcal{R}\mathcal{L}^{n_1}(\mathcal{L}\mathcal{R}\mathcal{L}^{n_1})^{n_2}}\\ &\quad = \{(\tilde{f}_{\mathcal{L}}^{n_1} \circ \tilde{f}_{\mathcal{R}} \circ \tilde{f}_{\mathcal{L}})^{n_2} \circ \tilde{f}_{\mathcal{L}}^{n_1} \circ \tilde{f}_{\mathcal{R}}(0) = 0\}\end{aligned} \tag{23b}$$

and for the second one by

$$\begin{aligned}&\xi_{\mathcal{L}\mathcal{R}\mathcal{L}^{n_1}(\mathcal{R}\mathcal{L}^{n_1})^{n_2}}\\ &\quad = \{(\tilde{f}_{\mathcal{L}}^{n_1} \circ \tilde{f}_{\mathcal{R}})^{n_2} \circ \tilde{f}_{\mathcal{L}}^{n_1} \circ \tilde{f}_{\mathcal{R}} \circ \tilde{f}_{\mathcal{L}}(0) = 0\}\end{aligned} \tag{24a}$$

$$\begin{aligned}&\xi_{\mathcal{R}\mathcal{L}^{n_1}\mathcal{L}\mathcal{R}\mathcal{L}^{n_1}(\mathcal{R}\mathcal{L}^{n_1})^{n_2-1}}\\ &\quad = \{(\tilde{f}_{\mathcal{L}}^{n_1} \circ \tilde{f}_{\mathcal{R}})^{n_2-1}\\ &\qquad \circ \tilde{f}_{\mathcal{L}}^{n_1} \circ \tilde{f}_{\mathcal{R}} \circ \tilde{f}_{\mathcal{L}} \circ \tilde{f}_{\mathcal{L}}^{n_1} \circ \tilde{f}_{\mathcal{R}}(0) = 0\}.\end{aligned} \tag{24b}$$

Note that although the so-called *map replacement technique* reported in [Avrutin *et al.*, 2010] is applicable for the explicit calculation of these bifurcation curves predominately if the functions $\tilde{f}_{\mathcal{L}}$ and $\tilde{f}_{\mathcal{R}}$ are linear, the implicit equations of the BCB curves associated with cycles with arbitrary complexity levels can always be obtained using this technique.

Similarly, between each two existence regions $\tilde{\mathcal{P}}_{\mathcal{LR}^{n_1}}$ and $\tilde{\mathcal{P}}_{\mathcal{LR}^{n_1+1}}$ of the cycles $\tilde{\mathcal{O}}_{\mathcal{LR}^{n_1}}$ and $\tilde{\mathcal{O}}_{\mathcal{LR}^{n_1+1}}$ there are two other infinite families of regions associated with the cycles of the complexity level two:

$$\begin{aligned}&\{\tilde{\mathcal{O}}_{\mathcal{RLR}^{n_1}(\mathcal{LR}^{n_1})^{n_2}} \,|\, n_i > 0, i = 1, 2\},\\ &\{\tilde{\mathcal{O}}_{\mathcal{LR}^{n_1}(\mathcal{RLR}^{n_1})^{n_2}} \,|\, n_i > 0, i = 1, 2\}.\end{aligned} \tag{25}$$

The BCB curves bounding the related periodicity regions are as given in Eqs. (23) and (24) by interchanging the symbols $\mathcal{L}$ and $\mathcal{R}$.

This process continues *ad infinitum*, so that between each two subsequent regions associated with cycles with the complexity level $k$ for any $k > 0$ there are two infinite families of regions associated with cycles of the complexity level $k+1$. The union of all regions of all complexity levels covers the region $\mathcal{P}_{\mathcal{B}}$ (in the neighborhood of $\mathcal{B}_{\sigma/\varrho}$) except for a Cantor set of particular bifurcation curves. For the parameters belonging to any of these curves the first return map is associated with an irrational rotation number and has a *Cantor set attractor*, which represents the closure of quasiperiodic trajectories [Keener, 1980; Ding & Fan, 1999].

The results obtained for the first return map (8) can easily be interpreted in terms of the original map (1). As the fixed points $\tilde{\mathcal{O}}_{\mathcal{L}}$ and $\tilde{\mathcal{O}}_{\mathcal{R}}$ of the first return map (8) correspond to the cycles $\mathcal{O}_\sigma$ and $\mathcal{O}_\varrho$ of map (1), the same correspondence can be provided for other cycles of the first return map (8). For example, the cycles of the complexity level one of the first return map (8) given in (19) correspond to the cycles

$$\{\mathcal{O}_{\varrho\sigma^{n_1}} \,|\, n_1 > 0\}, \quad \{\mathcal{O}_{\sigma\varrho^{n_1}} \,|\, n_1 > 0\} \tag{26}$$

of map (1). The related BCB equations are obtained (for any complexity level) replacing $\tilde{f}_{\mathcal{L}}$ and $\tilde{f}_{\mathcal{R}}$ by their definitions given in Eq. (8).

### 3.2. *Period incrementing structure*

Theorem 2 given in this subsection is proved by similar reasoning as in [Homburg, 1996] (Sec. 3.3) and in [Gardini & Tramontana, 2010; Gardini *et al.*, 2012] for particular classes of maps. A different proof is given in [Avrutin *et al.*, 2011].

**Theorem 2.** *Let $T$ in Eq. (10) satisfy the assumptions (H1)–(H4) given in Sec. 3. If for any $\zeta \in U(\mathcal{B})$ the function $T_{\mathcal{L}}(x;\zeta)$ is strictly increasing in $J_{\mathcal{L}}$ and $T_{\mathcal{R}}(x;\zeta)$ is strictly decreasing in $J_{\mathcal{R}}$, then $\mathcal{B}$ is an organizing center of a full period incrementing structure accumulating on $\xi_{\mathcal{L}}$.*

*Proof.* Let us consider region $\mathcal{P}_{\mathcal{B}}$ associated with no fixed points of $T$ in the no-escape interval $I = [T_{\mathcal{R}} \circ T_{\mathcal{L}}(0), T_{\mathcal{L}}(0)]$ as we can assume (eventually decreasing $U(\mathcal{B})$) that $[0, T_{\mathcal{L}}(0)] \subset J_{\mathcal{R}}$ and $[T_{\mathcal{R}} \circ T_{\mathcal{L}}(0), 0] \subset J_{\mathcal{L}}$. If the parameter values belong to the interior of $\mathcal{P}_{\mathcal{B}}$, then map $T$ has the absorbing interval $I = [T_{\mathcal{R}} \circ T_{\mathcal{L}}(0), T_{\mathcal{L}}(0)]$ where $T_{\mathcal{L}}(0) > 0$ and $T_{\mathcal{R}} \circ T_{\mathcal{L}}(0) < 0$.

Any point on the right side of $I$, that is, any $x_0 \in [0, T_{\mathcal{L}}(0)]$, is mapped into the left side in one iteration, that is, $x_1 = T_{\mathcal{R}}(x_0) \in [T_{\mathcal{R}} \circ T_{\mathcal{L}}(0), 0]$. Then, after a number $k$ of iterations by $T_{\mathcal{L}}$ the trajectory is back to the right side of $I$, that is, to the interval

$$J = [0, T_{\mathcal{L}}(0)]. \tag{27}$$

Thus, the properties of map $T$ in $I$ can be completely studied using its first return map, say $F_r(x)$, defined on the interval $J$. Namely, for each point $x \in J$, $x \neq 0$, its first return value $F_r(x)$ is given by $T_{\mathcal{L}}^k \circ T_{\mathcal{R}}(x)$ where $k \geq 1$ is the first integer such that $T_{\mathcal{L}}^k \circ T_{\mathcal{R}}(x) \in J$. It follows that any cycle of the map $T$ in $I$ is necessarily a maximal cycle, that is, a cycle with symbolic sequence $\mathcal{RL}^k$. The periodic point $x_0 > 0$ of such a cycle is obtained as a solution to the equation $T_{\mathcal{L}}^k \circ T_{\mathcal{R}}(x_0) = x_0$. A BCB of this cycle occurs when $x_0 = 0$, therefore, the equation

$$\xi_{\mathcal{RL}^k} = \{T_{\mathcal{L}}^k \circ T_{\mathcal{R}}(0) = 0\} \tag{28}$$

defines one BCB curve bounding the periodicity region $\mathcal{P}_{\mathcal{RL}^k}$. The other BCB of the same cycle occurs when the periodic point $x_k < 0$, which is a solution to $T_{\mathcal{L}}^{k-1} \circ T_{\mathcal{R}} \circ T_{\mathcal{L}}(x_k) = x_k$, collides with $x = 0$, so that the corresponding BCB curve is given by

$$\xi_{\mathcal{RLL}^{k-1}} = \{T_{\mathcal{L}}^{k-1} \circ T_{\mathcal{R}} \circ T_{\mathcal{L}}(0) = 0\}. \tag{29}$$

Notice that this equation also corresponds to the point $x_0 = T_{\mathcal{L}}(x_k)$ colliding with the right boundary of the interval $I$ (which is also the right boundary of $J$), that is, point $x_0 = T_{\mathcal{L}}(x_k)$ colliding with point $T_{\mathcal{L}}(0)$, and the BCB curve in (29) can also be written as $T_{\mathcal{L}}^k \circ T_{\mathcal{R}} \circ T_{\mathcal{L}}(0) = T_{\mathcal{L}}(0)$. The BCB curves given in Eqs. (28) and (29), bounding the periodicity region $\mathcal{P}_{\mathcal{RL}^k}$, issue from point $\mathcal{B}$ (as both equations are obviously satisfied in that point).

When the parameters belong to the curve $\xi_{\mathcal{L}}$ on the boundary of $\mathcal{P}_{\mathcal{B}}$ [let $A_{\mathcal{L}}$ be such a point,

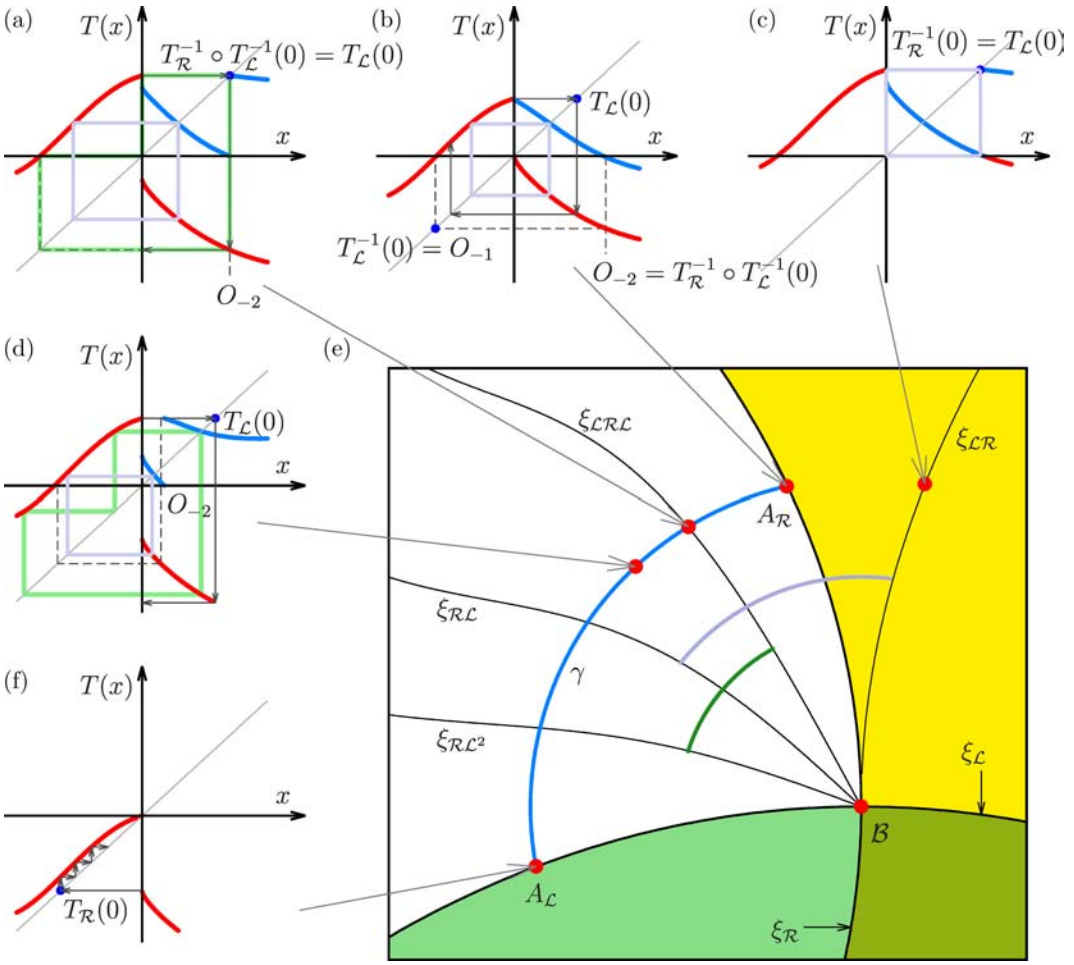


Fig. 5. Schematic structure of the parameter plane of map $T$ in the neighborhood $U(\mathcal{B})$ of the point $\mathcal{B}$ in the increasing–decreasing case. The graphs of $T$ are shown in red, and its first return map $F_r$ in blue.

as shown in Fig. 5(f)], map $T$ has an attracting fixed point $x^*_{\mathcal{L}} = 0$ which attracts all the points of $I = [T_{\mathcal{R}}(0), 0]$ as well as the points of a proper right neighborhood of $x = 0$ leading to trajectories with the symbolic sequence $\mathcal{RL}^\infty$. Diversely, when the parameters belong to the curve $\xi_{\mathcal{R}}$ on the boundary of $\mathcal{P}_{\mathcal{B}}$ (let $A_{\mathcal{R}}$ be such a point), the fixed point $x^*_{\mathcal{R}} = 0$ is not an attracting fixed point of $T$ [see Fig. 5(b)]. As the length of interval $T_{\mathcal{L}}^{-1}(J) = [O_{-1}, 0]$ is larger than the length of interval $J$, and the length of $T_{\mathcal{R}}^{-1} \circ T_{\mathcal{L}}^{-1}(J) = [0, O_{-2}]$ is larger as well, we have $O_{-2} = T_{\mathcal{R}}^{-1} \circ T_{\mathcal{L}}^{-1}(0) > T_{\mathcal{L}}(0)$. It follows that the first return map of $T$ in $J$ is given by $F_r(x) = T_{\mathcal{L}} \circ T_{\mathcal{R}}(x)$ and it has a globally attracting (in $J$) fixed point, corresponding to a 2-cycle of $T$.

It can be shown that the region $\mathcal{P}_{\mathcal{R}}$ in which the fixed point $x^*_{\mathcal{R}}$ exists and $x^*_{\mathcal{L}}$ does not exist is partially overlapped with the region $\mathcal{P}_{\mathcal{RL}}$ related to the 2-cycle. Indeed, bistability occurs if the inequality $T_{\mathcal{R}}^{-1}(0) < T_{\mathcal{L}}(0)$ holds. The BCB leading to the appearance of a 2-cycle coexisting with the fixed point $x^*_{\mathcal{R}}$ occurs for $T_{\mathcal{R}}^{-1}(0) = T_{\mathcal{L}}(0)$ [see Fig. 5(c)]. This condition is obviously equivalent to the one given in (29) for $k = 1$, that is,

$$\xi_{\mathcal{LR}} = \{T_{\mathcal{R}} \circ T_{\mathcal{L}}(0) = 0\}. \tag{30}$$

The BCB curve $\xi_{\mathcal{LR}}$ issues from point $\mathcal{B}$ and necessarily enters the region $\mathcal{P}_{\mathcal{R}}$.

Now let us consider an arc $\gamma$ belonging to the region $\mathcal{P}_{\mathcal{B}}$ connecting $A_{\mathcal{R}}$ with $A_{\mathcal{L}}$ [see Fig. 5(e)]. Using the first return map $F_r(x)$ defined on the interval $J$ we can show that when the parameter point moves from $A_{\mathcal{R}}$ towards $A_{\mathcal{L}}$ along the arc $\gamma$, all the regions $\mathcal{P}_{\mathcal{RL}^k}$ must be crossed. Moreover, any two consecutive regions $\mathcal{P}_{\mathcal{RL}^k}$ and $\mathcal{P}_{\mathcal{RL}^{k+1}}$ partially overlap, which leads to bistability. In fact, at point $A_{\mathcal{R}}$ (which corresponds to the BCB curve $\xi_{\mathcal{R}}$ associated with the disappearance of the fixed point $x^*_{\mathcal{R}}$), a 2-cycle with the symbolic sequence $\mathcal{RL}$ exists and, as we have seen, the condition

$O_{-2} = T_{\mathcal{R}}^{-1} \circ T_{\mathcal{L}}^{-1}(0) > T_{\mathcal{L}}(0)$ holds [see Fig. 5(b)], so that for parameter values close to point $A_{\mathcal{R}}$ on the arc $\gamma$ the first return map of $T$ in the interval $J$ is given by

$$F_r(x) = T_{\mathcal{L}} \circ T_{\mathcal{R}}(x) \tag{31}$$

and the 2-cycle of the map $T$ is globally attracting in $I$. Moving the parameter point along the arc $\gamma$ a BCB occurs when the condition $T_{\mathcal{R}}^{-1} \circ T_{\mathcal{L}}^{-1}(0) = T_{\mathcal{L}}(0)$ is satisfied [see Fig. 5(a)], which defines a BCB curve

$$\xi_{\mathcal{LRL}} = \{T_{\mathcal{L}} \circ T_{\mathcal{R}} \circ T_{\mathcal{L}}(0) = 0\} \tag{32}$$

associated with the appearance of a 3-cycle of $T$, with the symbolic sequence $\mathcal{RL}^2$ [see Fig. 5(e)]. As the parameter point continues to move along the arc $\gamma$ the preimage of the discontinuity point $O_{-2} = T_{\mathcal{R}}^{-1} \circ T_{\mathcal{L}}^{-1}(0) \in J$, so an arc $\gamma$ must exist such that the first return map is defined as

$$F_r(x) = \begin{cases} T_0(x) = T_{\mathcal{L}} \circ T_{\mathcal{R}}(x) \\ \qquad\qquad \text{if } 0 \le x < O_{-2} \\ T_1(x) = T_{\mathcal{L}}^2 \circ T_{\mathcal{R}}(x) \\ \qquad\qquad \text{if } O_{-2} < x \le T_{\mathcal{L}}(0). \end{cases} \tag{33}$$

From $T_0(O_{-2}) = T_{\mathcal{L}} \circ T_{\mathcal{R}}(O_{-2}) = 0$ and $T_1(O_{-2}) = T_{\mathcal{L}}^2 \circ T_{\mathcal{R}}(O_{-2}) = T_{\mathcal{L}}(0)$ it follows that each of the two decreasing branches of $F_r(x)$ must have a stable fixed point, so that there is a coexistence of a stable 2-cycle and a stable 3-cycle of $T$.

Now let us show that in $\mathcal{P}_{\mathcal{B}}$ there exist periodicity regions $\mathcal{P}_{\mathcal{RL}^k}$ for any $k > 0$, issuing from $\mathcal{B}$, accumulating on the curve $\xi_{\mathcal{L}}$, and any two consecutive regions partially overlap.

For parameters in $\mathcal{P}_{\mathcal{B}}$ the first return map $F_r(x)$ of $T$ in $J$ is either continuous, defined via one unique decreasing function, or it has at most one discontinuity point in $J$, being defined via two decreasing functions. In fact, the discontinuity points of $F_r(x)$ are given by the preimages of $x = 0$ in the interval $J$. The function $T_{\mathcal{L}}(x)$ and hence $T_{\mathcal{L}}^k(x)$ are increasing, thus invertible in $I$, and the function $T_{\mathcal{R}}(x)$ is decreasing thus invertible in $I$. Let $O_{-(k+1)}$ be the preimage of $x = 0$ belonging to the right side of $I$ closest to $x = 0$. It is given by

$$O_{-(k+1)} = T_{\mathcal{R}}^{-1} \circ T_{\mathcal{L}}^{-k}(0) \tag{34}$$

for some $k \ge 1$. The functions $T_{\mathcal{R}}^{-1} \circ T_{\mathcal{L}}^{-k}(x)$ are expanding, so that, apart from the bifurcations occurring at $O_{-(k+1)} = T_{\mathcal{L}}(0)$ (which corresponds to $T_{\mathcal{R}}^{-1} \circ T_{\mathcal{L}}^{-k}(0) = T_{\mathcal{L}}(0)$, that is, $T_{\mathcal{L}}^k \circ T_{\mathcal{R}} \circ T_{\mathcal{L}}(0) = 0$, related to the BCB of a $(k+2)$-cycle as given in Eq. (29) with $k$ in place of $k-1$), and $O_{-(k+1)} = 0$ [which corresponds to $T_{\mathcal{R}}^{-1} \circ T_{\mathcal{L}}^{-k}(0) = 0$ that is $T_{\mathcal{L}}^k \circ T_{\mathcal{R}}(0) = 0$, which is the bifurcation of a $(k+1)$-cycle as given in Eq. (28)], we have only two possibilities.

(a) If $O_{-(k+1)} > T_{\mathcal{L}}(0)$, then map $F_{\mathcal{R}}(x)$ is defined as

$$F_{\mathcal{R}}(x) = T_{\mathcal{L}}^k \circ T_{\mathcal{R}}(x) \tag{35}$$

for $x \in J$ [see Fig. 6(a)].

(b) If $0 < O_{-(k+1)} < T_{\mathcal{L}}(0)$ (given that at most one preimage can belong to $J$), then map $F_{\mathcal{R}}(x)$ is defined as

$$F_{\mathcal{R}}(x) = \begin{cases} T_0(x) = T_{\mathcal{L}}^k \circ T_{\mathcal{R}}(x) \\ \qquad\qquad \text{if } 0 \le x < O_{-(k+1)} \\ T_1(x) = T_{\mathcal{L}}^{k+1} \circ T_{\mathcal{R}}(x) \\ \qquad\qquad \text{if } O_{-(k+1)} < x \le T_{\mathcal{L}}(0). \end{cases} \tag{36}$$

In this case, $T_0(O_{-(k+1)}) = T_{\mathcal{L}}^k \circ T_{\mathcal{R}}(O_{-(k+1)}) = 0$ implies the existence of a fixed point of $T_0$, that is a stable cycle with symbolic sequence $\mathcal{RL}^k$ for $T$. Meanwhile, $T_1(O_{-(k+1)}) = T_{\mathcal{L}}^{k+1} \circ T_{\mathcal{R}}(O_{-(k+1)}) = T_{\mathcal{L}}(0)$ implies the existence of a fixed point of $T_1$ in $J$, that is a stable cycle with symbolic sequence $\mathcal{RL}^{k+1}$ for $T$. Hence, two stable cycles of $T$ coexist [see Fig. 6(b)].

Note that the expansivity of the function $T_{\mathcal{R}}^{-1} \circ T_{\mathcal{L}}^{-(k+1)}$ implies that at a bifurcation defined by $O_{-(k+1)} = 0$ we have $O_{-(k+2)} > T_{\mathcal{L}}(0)$.

So, as the parameter point moves along the arc $\gamma$ inside the region $\mathcal{P}_{\mathcal{B}}$ approaching $A_{\mathcal{L}}$ (where the trajectories have the symbolic sequence $\mathcal{RL}^\infty$), all the periodicity regions $\mathcal{P}_{\mathcal{RL}^k}$ are necessarily crossed. In fact, when the parameter point approaches $A_{\mathcal{L}}$ the first preimage of the origin belonging to $J$, $O_{-(k+1)}$, occurs for values of $k$ which become larger and larger, approaching infinity, and the cases (a) and (b) defined above occur for each $k$. Therefore, for each $k$ there exists a part of the region $\mathcal{P}_{\mathcal{RL}^n}$ in which a cycle with the symbolic sequence $\mathcal{RL}^k$ is globally attracting, and a part in which this cycle coexists with a cycle with the symbolic sequence $\mathcal{RL}^{k+1}$.

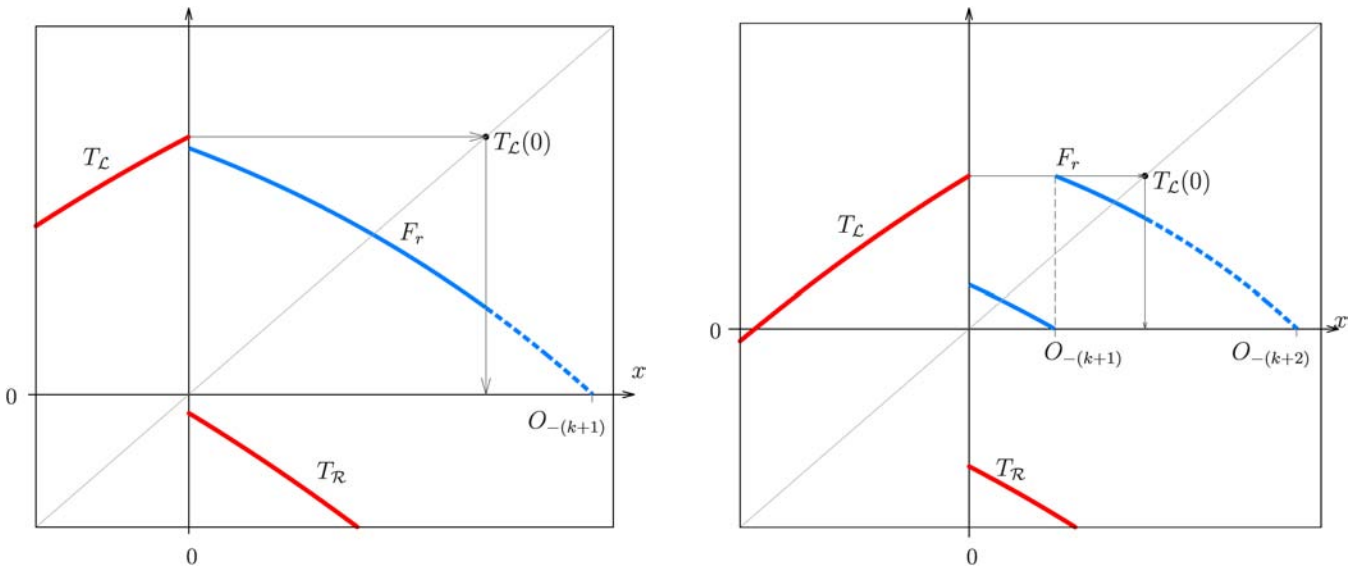


Fig. 6. First return map $F_r$ in the cases in which map $T$ has (a) a unique cycle and (b) two cycles.

Summarizing: let $O_{-(k+1)} = T_{\mathcal{R}}^{-1} \circ T_{\mathcal{L}}^{-k}(0)$ be the preimage of the origin in $J$. Then

- either $O_{-(k+1)} > T_{\mathcal{L}}(0)$, in which case there exists a unique attracting cycle with the symbolic sequence $\mathcal{RL}^k$,
- or $O_{-(k+1)} \in [0, T_{\mathcal{L}}(0)]$, in which case there are two coexisting attracting cycles, with symbolic sequences $\mathcal{RL}^k$ and $\mathcal{RL}^{k+1}$.

The BCB curves associated with the cycles are given in Eqs. (28) and (29) bounding the regions $\mathcal{P}_{\mathcal{RL}^k}$ for all $k$, and accumulating on the BCB curve $\xi_{\mathcal{L}}$ as $k$ tends to infinity.

If function $T_{\mathcal{L}}$ is decreasing and function $T_{\mathcal{R}}$ is increasing, the same results are valid with $\mathcal{L}$ and $\mathcal{R}$ interchanged. ■

Consider two cycles $\mathcal{O}_\sigma$ and $\mathcal{O}_\varrho$ of the map (1), and let $\mathcal{B}_{\sigma/\varrho}$ be a point of a transverse intersection of two BCB curves $\xi_\sigma^{\mathcal{L}}$ and $\xi_\varrho^{\mathcal{R}}$, at which the assumptions of Theorem 2 are satisfied by the first return map $\tilde{f}$ given in (8). Then point $\mathcal{B}_{\sigma/\varrho}$ is an organizing center of a period incrementing structure. The bifurcation structure in the parameter plane around point $\mathcal{B}_{\sigma/\varrho}$ is shown schematically in Fig. 7. This bifurcation structure is formed by an infinite family of periodicity regions $\tilde{\mathcal{P}}_{\mathcal{RL}^n}$, $n > 0$, of stable cycles

$$\{\tilde{\mathcal{O}}_{\mathcal{RL}^n} \,|\, n > 0\} \tag{37}$$

pairwise partially overlapping for any $n > 0$. Moreover, for $n \to \infty$, the regions $\tilde{\mathcal{P}}_{\mathcal{RL}^n}$ accumulate towards the BCB curve $\xi_\sigma^{\mathcal{L}}$. Accordingly, for the original map (1) this family corresponds to the cycles

$$\{\mathcal{O}_{\varrho\sigma^n} \,|\, n > 0\}. \tag{38}$$

### 3.3. *Coupling bifurcation structure*

Theorem 3, proved in this section, is the simplest case:

**Theorem 3.** *Let $T$ in Eq. (10) satisfy the assumptions (H1)–(H4) given in Sec. 3. If for any $\zeta \in U(\mathcal{B})$ the functions $T_{\mathcal{L}}(x;\zeta)$ and $T_{\mathcal{R}}(x;\zeta)$ are strictly decreasing in $I_{\mathcal{L}}$ and $I_{\mathcal{R}}$, respectively, then a coupling structure issues from $\mathcal{B}$.*

*Proof.* Let us consider the region $\mathcal{P}_{\mathcal{B}}$ associated with no fixed points of $T$. When the parameters belong to the region $\mathcal{P}_{\mathcal{B}}$ (boundaries included) each point $x > 0$ in a neighborhood of $x = 0$ is mapped into the left side in one iteration. It follows that the properties of $T$ can be studied using the first return map, say $F_r(x)$, of $T$ on the right side, which is necessarily defined as

$$F_r(x) = T_{\mathcal{L}} \circ T_{\mathcal{R}}(x). \tag{39}$$

From the assumptions given above we have $0 \leq F_r'(x)|_{x=0} < 1$ thus $F_r(x)$ is increasing and contracting in a right neighborhood of $x = 0$, with

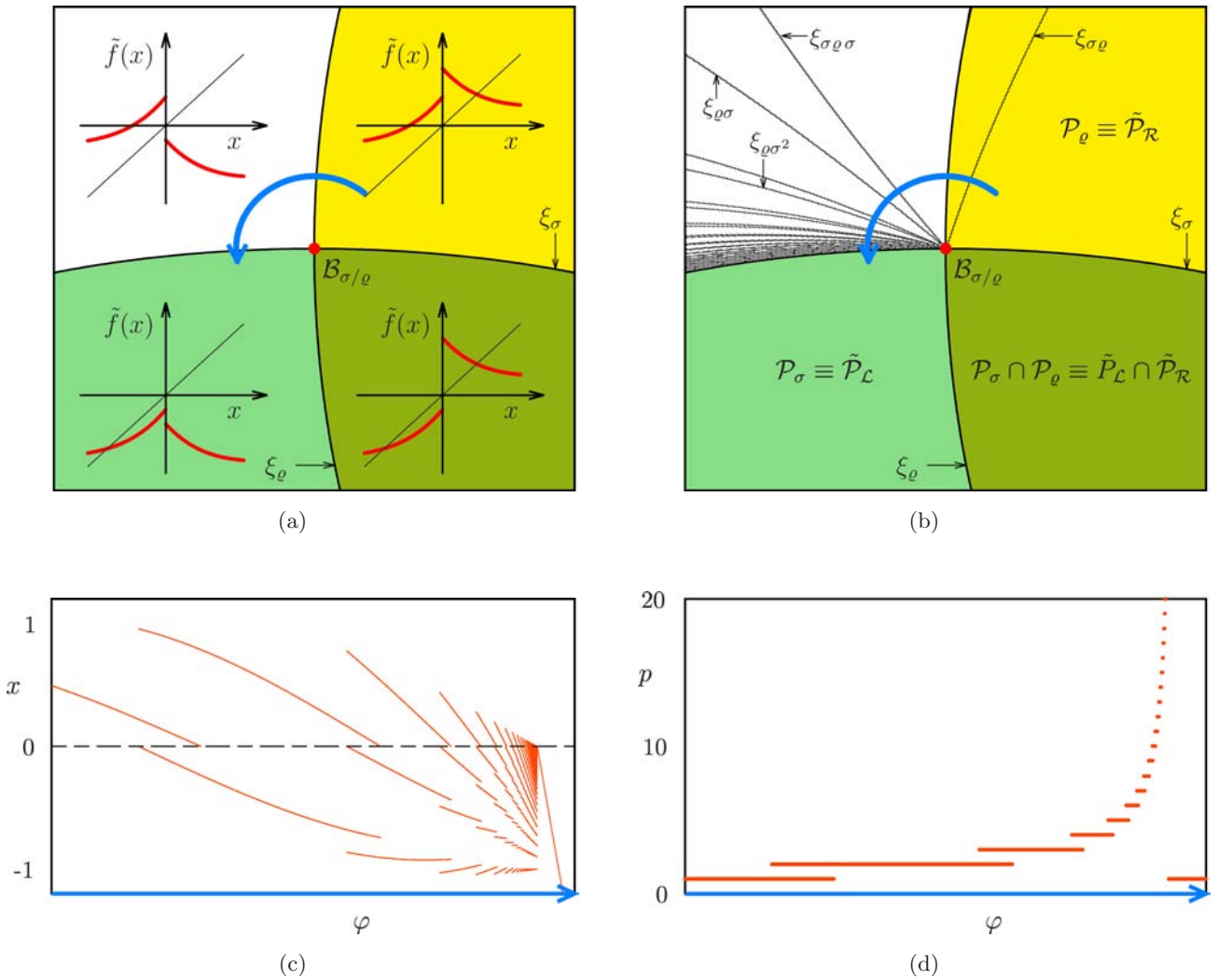


Fig. 7. In (a) and (b) the shapes of the first return map (8) in the increasing–decreasing configuration and the bifurcation structures close to the intersection point of the BCB curves $\tilde{\xi}_\mathcal{L}$ and $\tilde{\xi}_\mathcal{R}$ are shown schematically. (c) and (d) show the associated bifurcation and period ($p$) diagrams, respectively, under variation of the angle $\varphi$ along the arc marked blue in (a) and (b).

$F_r(0) > 0$. Therefore, there exists a suitable region in a neighborhood of $\mathcal{B}$ such that a stable fixed point of $F_r$ exists, representing a stable 2-cycle of $T$, with the symbolic sequence $\mathcal{RL}$ [see Fig. 8(d)]. As such a 2-cycle also exists for parameters belonging to each of the BCB curves $\xi_\mathcal{L}$ and $\xi_\mathcal{R}$, the curves associated with its existence region, given by

$$\xi_{\mathcal{RL}} = \{T_\mathcal{L} \circ T_\mathcal{R}(0) = 0\} \tag{40a}$$

$$\xi_{\mathcal{LR}} = \{T_\mathcal{R} \circ T_\mathcal{L}(0) = 0\} \tag{40b}$$

issue from parameter point $\mathcal{B}$ and enter regions $\mathcal{P}_\mathcal{L}$ and $\mathcal{P}_\mathcal{R}$ of the stable fixed points $x^*_\mathcal{L}$ and $x^*_\mathcal{R}$ (see Fig. 8).

In the parameter region in $U(\mathcal{B})$ bounded by the BCB curves $\xi_\mathcal{R}$ and $\xi_{\mathcal{LR}}$ we can define the first return map on the right side of $x = 0$, which is given by

$$F_r(x) = \begin{cases} T_0(x) = T_\mathcal{R}(x) & \text{if } 0 \le x < O_{-1} \\ T_1(x) = T_\mathcal{L} \circ T_\mathcal{R}(x) & \text{if } x > O_{-1} \end{cases} \tag{41}$$

where $O_{-1} = T_\mathcal{R}^{-1}(0) > 0$ [see Fig. 8(b)]. In fact, on the BCB curve $\xi_\mathcal{R}$ we have $O_{-1} = 0$ and $T_\mathcal{L}(0) > O_{-1}$, so that for parameters close to $\xi_\mathcal{R}$ we have $O_{-1} > 0$ and $T_\mathcal{L}(0) > O_{-1}$. From $T_\mathcal{R}(0) > 0$ and $T_\mathcal{R}(O_{-1}) = 0$ it follows that a fixed point of the decreasing branch $T_0(x) = T_\mathcal{R}(x)$ exists, which is the stable fixed point $x^*_\mathcal{R}$. From $T_\mathcal{L} \circ T_\mathcal{R}(O_{-1}) = T_\mathcal{L}(0) > O_{-1}$ the increasing and contracting branch $T_1(x)$ leads to the existence of

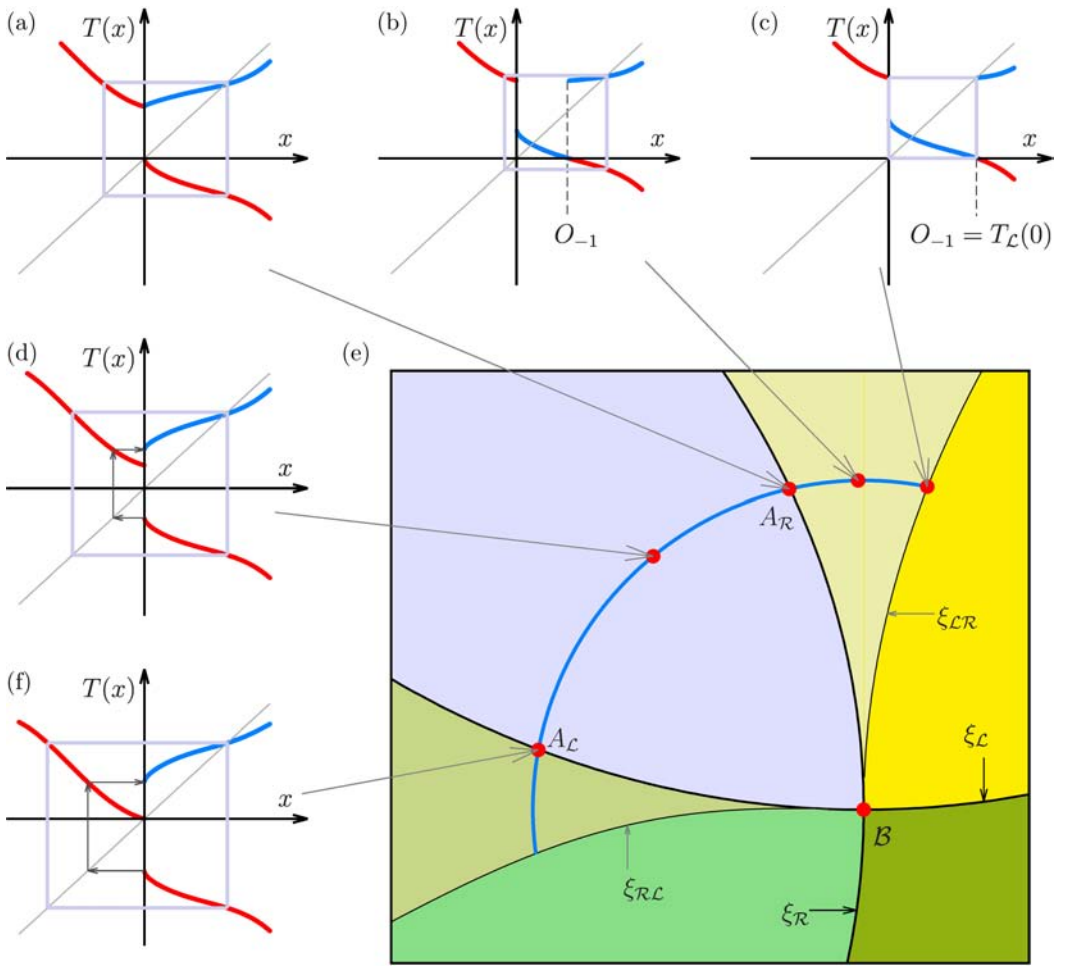


Fig. 8. Schematic structure of the parameter plane of map $T$ in the neighborhood $U(\mathcal{B})$ of point $\mathcal{B}$ in the decreasing–decreasing case. The graphs of $T$ are shown in red, and its first return map $F_r$ in blue.

a fixed point, so that the stable fixed point $x^*_{\mathcal{R}}$ coexists with a stable 2-cycle of $T$. This 2-cycle disappears when $T_{\mathcal{L}}(0) = O_{-1}$ [see Fig. 8(c)], that is, $T_{\mathcal{R}} \circ T_{\mathcal{L}}(0) = 0$, corresponding to the BCB curve $\xi_{\mathcal{LR}}$ which is the boundary of the periodicity region $\mathcal{P}_{\mathcal{RL}}$ overlapping with $\mathcal{P}_{\mathcal{R}}$.

Similarly, in the parameter region bounded by the BCB curves $\xi_{\mathcal{L}}$ and $\xi_{\mathcal{RL}}$ we can define the first return map on the left side of $x = 0$:

$$F_\ell(x) = \begin{cases} T_0(x) = T_{\mathcal{R}} \circ T_{\mathcal{L}}(x) & \text{if } x < O_{-1} \\ T_1(x) = T_{\mathcal{L}}(x) & \text{if } O_{-1} < x \le 0 \end{cases} \tag{42}$$

where $O_{-1} = T_{\mathcal{L}}^{-1}(0)$. The conditions $T_{\mathcal{L}}(O_{-1}) = 0$ and $T_{\mathcal{L}}(0) < 0$ imply the existence of a stable fixed point $x^*_{\mathcal{L}}$ of the decreasing branch $T_1(x) = T_{\mathcal{L}}(x)$. From $T_{\mathcal{R}} \circ T_{\mathcal{L}}(O_{-1}) = T_{\mathcal{R}}(0) < O_{-1}$ the increasing and contracting branch $T_0(x)$ leads to a fixed point, so that the stable fixed point $x^*_{\mathcal{L}}$ coexists with a stable 2-cycle of $T$. ■

Consider two cycles $\mathcal{O}_\sigma$ and $\mathcal{O}_\varrho$ of the map (1), and let $\mathcal{B}_{\sigma/\varrho}$ be a point of a transverse intersection of two BCB curves $\xi^{\mathcal{L}}_\sigma$ and $\xi^{\mathcal{R}}_\varrho$, at which the assumptions of Theorem 3 hold for the first return map $\tilde{f}$ given in (8). Then from the point $\mathcal{B}_{\sigma/\varrho}$ only the periodicity region of the coupled cycle $\mathcal{O}_{\sigma\varrho}$ issues. The so-called coupling bifurcation structure in the parameter plane around point $\mathcal{B}_{\sigma/\varrho}$ is shown schematically in Fig. 9.

In one of the quadrants, two fixed points $\tilde{\mathcal{O}}_{\mathcal{L}}$ and $\tilde{\mathcal{O}}_{\mathcal{R}}$ of map (8) coexist; each of the adjacent quadrants consists of two regions: in one the fixed point exists alone, and in the second one it coexists with the attracting 2-cycle $\tilde{\mathcal{O}}_{\mathcal{LR}}$. In the remaining quadrant $\mathcal{P}_{\mathcal{B}}$ only the attracting 2-cycle $\tilde{\mathcal{O}}_{\mathcal{LR}}$ exists. Clearly, for the original map (1) this corresponds to

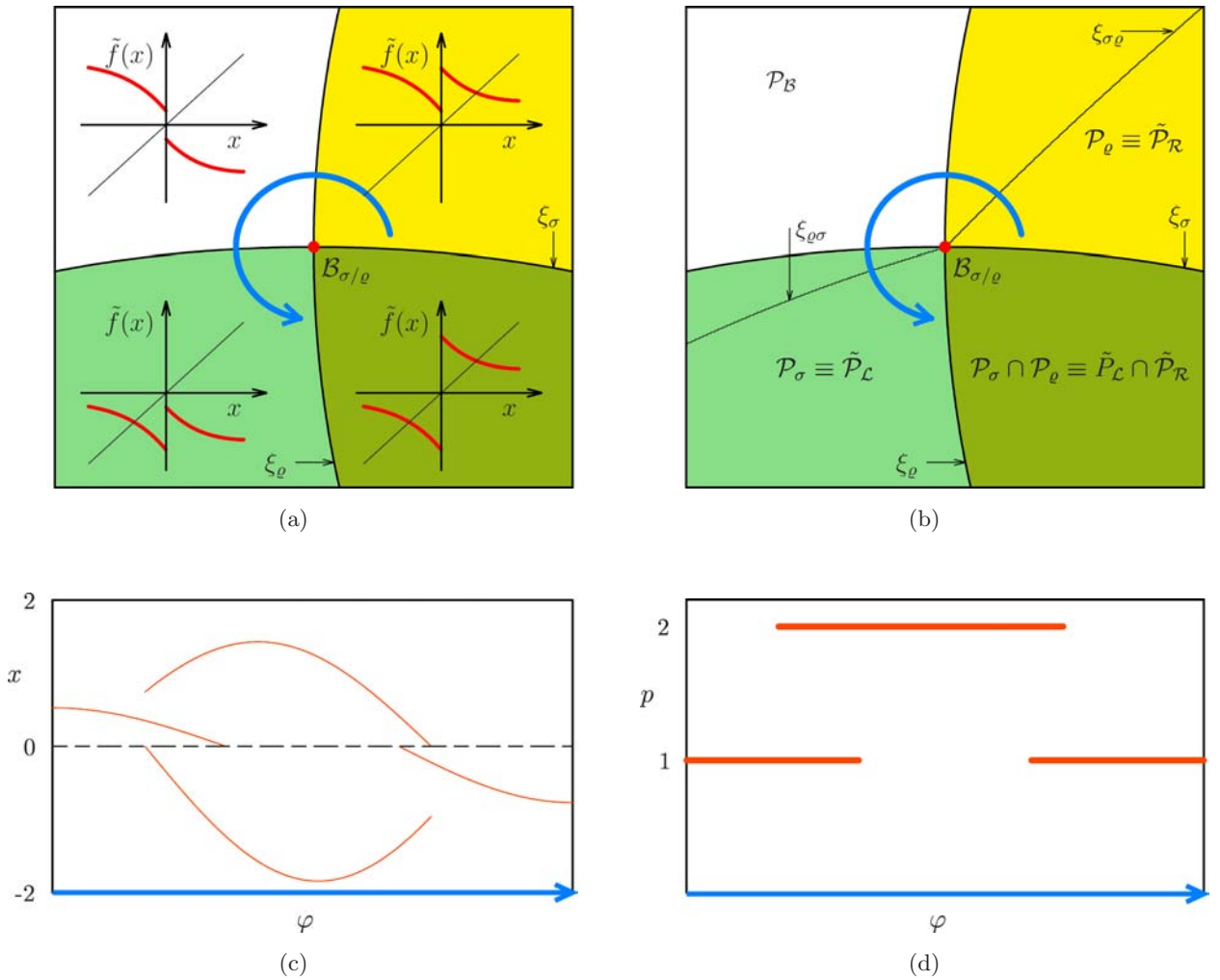


Fig. 9. In (a) and (b) the shapes of the first return map (8) in the decreasing–decreasing configuration and the bifurcation structures close to the intersection point of the border collision bifurcation curves $\tilde{\xi}_\mathcal{L}$ and $\tilde{\xi}_\mathcal{R}$ are shown schematically. (c) and (d) show the associated bifurcation and period ($p$) diagrams, respectively, under variation of the angle $\varphi$ along the arc marked blue in (a) and (b).

the attracting cycles $\mathcal{O}_\sigma$ and $\mathcal{O}_\varrho$ and the attracting cycle $\mathcal{O}_{\sigma\varrho}$.

## 4. Lorenz-Like Flows and Associated 1D Maps

Recall that three-dimensional Lorenz-like flows satisfy the following two conditions:

- The flow has a saddle point at the origin with *real* eigenvalues denoted $\lambda^{ss}$, $\lambda^s$ and $\lambda^u$, with $\lambda^{ss} < \lambda^s < 0 < \lambda^u$, so that the saddle has a stable two-dimensional manifold and an unstable one-dimensional manifold.
- Homoclinic orbits of the flow are of the butterfly type as shown in Fig. 10(a), and not of the figure-eight type [see Fig. 10(b)].[10]

An example of the flow which satisfies the conditions mentioned above is the original Lorenz flow introduced in [Lorenz, 1963]. A different example introduced in [Lyubimov *et al.*, 1989] extends the original Lorenz model:

$$\begin{aligned} \dot{x} &= \sigma(y - x) + \sigma D y(z - R) \\ \dot{y} &= Rx - y - xz \\ \dot{z} &= xy - bz + ax. \end{aligned} \tag{43}$$

[10]For the difference between the cases of butterfly type and figure-eight type orbits we refer to [Ghrist, 2000].

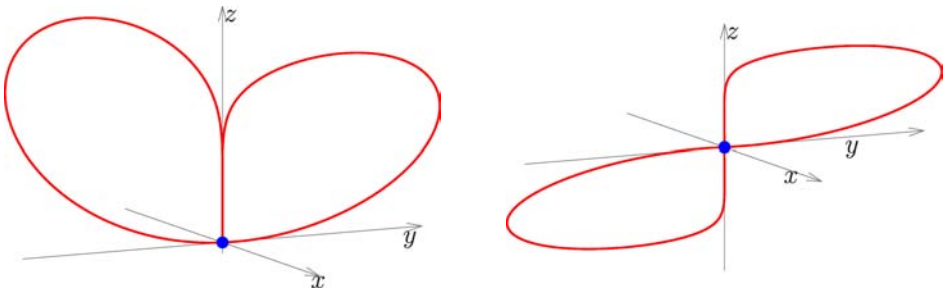


(a) (b)

Fig. 10. Standard configurations of flows: (a) a butterfly structure and (b) a figure-eight structure.

The origin is an equilibrium of this flow. For the commonly considered values of the parameters $\sigma$, $R$ and $b$ (as, for example, in Fig. 12) it represents a saddle with a two-dimensional stable and a 1D unstable manifold.

It is well-known (see [Sparrow, 1982; Glendinning, 1988; Lyubimov *et al.*, 1989; Homburg, 1996; Zaks, 1993]) that dynamic properties of Lorenz-like flows depend strongly on the saddle-index $\gamma$ of the origin, which is defined by

$$\gamma = -\frac{\lambda^s}{\lambda^u}. \tag{44}$$

For example, the saddle-index of the equilibrium at the origin of (43) is given by

$$\gamma = \frac{b}{-\dfrac{\sigma+1}{2} + \sqrt{\left(\dfrac{\sigma-1}{2}\right)^2 + \sigma R(1-D\sigma)}}. \tag{45}$$

The saddle-index $\gamma$ appears in the following 1D first return map of Lorenz-like flows:

$$x_{n+1} = g(x_n) = \begin{cases} g_{\mathcal{L}}(x_n) = \mu_{\mathcal{L}} - a_{\mathcal{L}}|x_n|^{\gamma} \\ \qquad\qquad + \text{h.o.t.} & \text{if } x_n < 0 \\ g_{\mathcal{R}}(x_n) = -\mu_{\mathcal{R}} + a_{\mathcal{R}}|x_n|^{\gamma} \\ \qquad\qquad + \text{h.o.t.} & \text{if } x_n > 0 \end{cases} \tag{46}$$

which is usually approximated by

$$x_{n+1} = g(x_n) = \begin{cases} g_{\mathcal{L}}(x_n) = \mu_{\mathcal{L}} - a_{\mathcal{L}}|x_n|^{\gamma} & \text{if } x_n < 0 \\ g_{\mathcal{R}}(x_n) = -\mu_{\mathcal{R}} + a_{\mathcal{R}}|x_n|^{\gamma} & \text{if } x_n > 0. \end{cases} \tag{47}$$

Map $g$ describes the return of the orbits of the original flow started at the top surface of an infinitesimally small box around the equilibrium at the origin back to this surface. Here the switching value $x = 0$ of map $g$ corresponds to the equilibrium at the origin of the flow. Therefore, for the sake of completeness, in Eqs. (46) and (47) one could add $g(0) = 0$. However, it is known that the definition of the system at the border does not influence the bifurcation structures in the parameter space of the map, while the values $g_{\mathcal{L}}(0)$ and $g_{\mathcal{R}}(0)$ (so-called critical points) are important for the description of the bifurcation structures.

Regarding the relation between the parameters of map $g$ defined by Eq. (47) and the parameters of the underlying flow, we have that for a particular system the value of the saddle-index $\gamma$ can be calculated analytically. In much of the literature, the values $\gamma = \frac{1}{2}$ and $\gamma = 2$ are considered to be representatives for the cases of maps which are, respectively, expanding ($0 < \gamma < 1$) and contracting ($\gamma > 1$) around the origin. Indeed, it is proved in [Labarca & Moreira, 2001] (resp. [Labarca & Moreira, 2010]) that map (47) with any $0 < \gamma < 1$ (resp. $\gamma > 1$) is topologically conjugate to the map with $\gamma = \frac{1}{2}$ (resp. $\gamma = 2$). It is known that the dynamics in these cases are basically different.

The dependency of the other parameters $a_{\mathcal{L}}$, $a_{\mathcal{R}}$ and $\mu_{\mathcal{L}}$, $\mu_{\mathcal{R}}$ of $g$ on the parameters of the flow cannot be derived analytically. However, it can be shown that the signs of the parameters $a_{\mathcal{L}}$, $a_{\mathcal{R}}$ depend on the rotation (twist) of the orbits around the unstable 1D manifold. In particular, the so-called nontwisted, single-twisted and double-twisted configurations (see [Ghrist & Holmes, 1993]) lead to the cases in which $a_{\mathcal{L}}$, $a_{\mathcal{R}}$ are both positive, have different signs, and are both negative, respectively. Accordingly, we have to distinguish between the six cases illustrated in Fig. 11. The cases shown

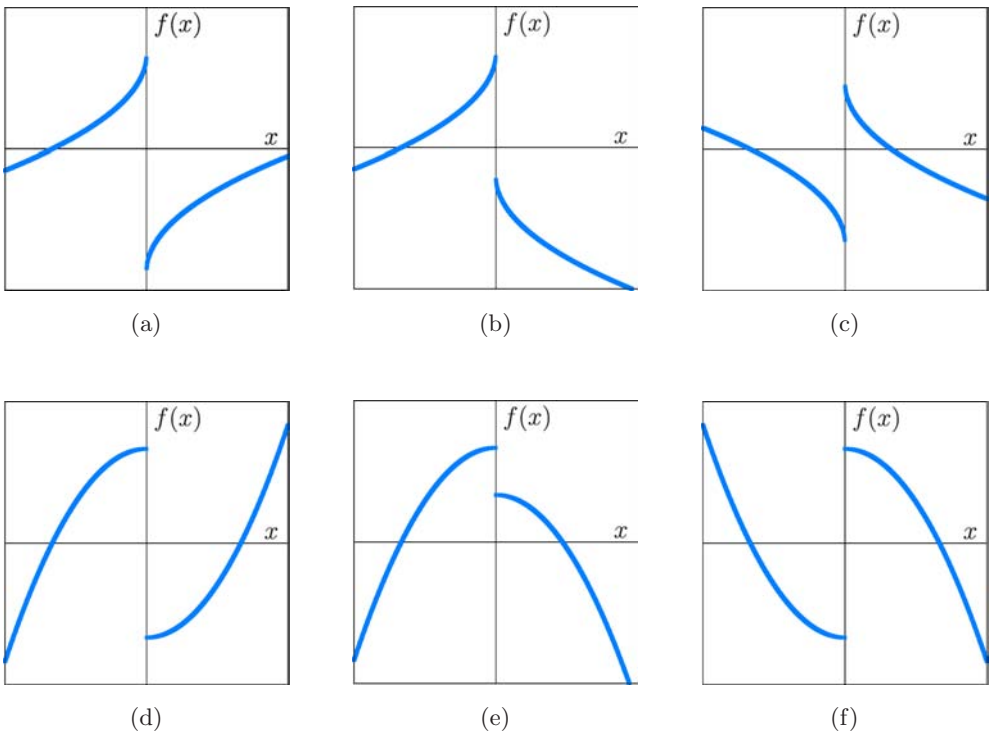


Fig. 11. Map (47) in the cases corresponding to the saddle index $0 < \gamma < 1$ (a, b, c) and $\gamma > 1$ (d, e, f). The signs of the parameters $a_{\mathcal{L}}$, $a_{\mathcal{R}}$ correspond to the nontwisted (a, d), single-twisted (b, e) and double-twisted (c, f) cases.

in Figs. 11(a)–11(c) correspond to the saddle-index $0 < \gamma < 1$, and those shown in Figs. 11(d)–11(f) to $\gamma > 1$. The nontwisted, single-twisted and double-twisted cases are shown in Figs. 11(a) and 11(d), Figs. 11(b) and 11(e), Figs. 11(c) and 11(f), respectively.

The one-to-one correspondence between limit cycles in the Lorenz-like flow and periodic orbits, or cycles, in map $g$ leads, in particular, to the fact that if a cycle of map (47) undergoes a BCB (that means, one of its points collides with the border point $x = 0$), then the underlying limit cycle of the flow merges with the origin and becomes a homoclinic orbit of the saddle of the flow.

This correspondence is illustrated in Fig. 12 for a stable limit cycle of the flow (43) which corresponds to a 2-cycle of map (47). It can be calculated straightforwardly by Eq. (45) that at the related parameter values the origin has the saddle-index $\gamma = 1.5$.

In Fig. 12(a) a limit cycle of (43) is shown for the parameter values in the middle of its existence region. When the parameter values are moved closer to the boundary of this region [see Fig. 12(b)], one of the loops of the limit cycle moves towards the saddle at the origin, and the corresponding point of the 2-cycle of map $g$ moves towards the discontinuity point $x = 0$. For the parameter values belonging to the boundary of the existence region of the limit cycle, as shown in Fig. 12(c), the limit cycle merges with the saddle at the origin and becomes a homoclinic orbit. For the corresponding parameter values one point of the 2-cycle of map $g$ merges with the discontinuity point $x = 0$, that means the 2-cycle undergoes a BCB.

Note that considering the first return map (8) related to any two cycles $\mathcal{O}_\sigma$ and $\mathcal{O}_\varrho$ of map $g$ in Eq. (47) the derivatives of the functions $\tilde{f}_{\mathcal{L}}(x)$ and $\tilde{f}_{\mathcal{R}}(x)$ at $x = 0$ are $s_{\mathcal{L}} = s_{\mathcal{R}} = 0$ in the contracting case (that means $\gamma > 1$) or $s_{\mathcal{L}} = s_{\mathcal{R}} = \pm\infty$ in the expanding case (that means $0 < \gamma < 1$). As we shall see, in such cases as well, what really matters for the classification of the bifurcation structures is whether functions $\tilde{f}_{\mathcal{L}}(x)$ and $\tilde{f}_{\mathcal{R}}(x)$ are contracting or expanding and increasing or decreasing. For map (47) with $\gamma > 1$ it can easily be seen that any cycle at the moment of a BCB is necessarily stable, and hence any codimension-2 BCB point is associated with stable cycles and belongs to the class of maps considered in Sec. 2. By contrast all organizing centers in map (47) for $0 < \gamma < 1$ are related to BCBs of unstable cycles.

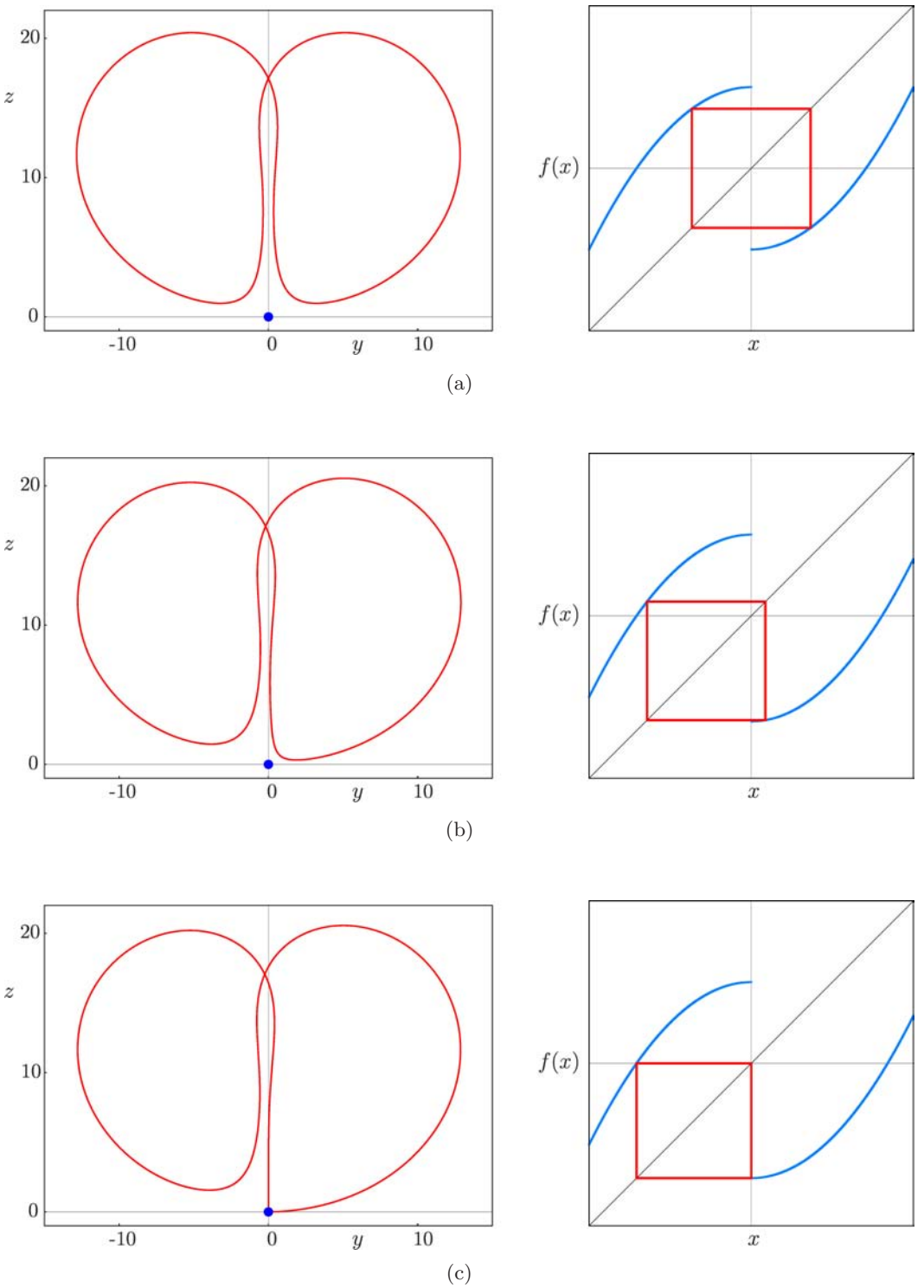


Fig. 12. Correspondence between a homoclinic bifurcation of the saddle at the origin in the flow (43) and the related BCB of a 2-cycle in map (47). Parameters: $\sigma = 10$, $R = 13.3$, $b = \frac{8}{3}$, $D = 0.05669283$, (a) $a = 0$, (b) $a = 0.1$ and (c) $a = 0.1565$.

### 4.1. *Increasing–increasing case*

Theorem 1 applies to map (47) in the case $\gamma > 1$, $a_{\mathcal{L}} > 0$, $a_{\mathcal{R}} > 0$ which corresponds to the non-twisted case of the underlying flows. The bifurcation structure issuing from point $\mathcal{B}_{\mathcal{L}/\mathcal{R}}$ marked in Fig. 13 is already known (see for example [Turaev & Shil'nikov, 1987 (Russian version 1986); Gambaudo *et al.*, 1986; Procaccia *et al.*, 1987; Lyubimov *et al.*, 1989; Homburg, 1996; Ghrist & Holmes, 1994]). We present it in Fig. 13 using the following topology-preserving mapping of the parameters $\mu_{\mathcal{L}}$, $\mu_{\mathcal{R}}$:

$$\mathcal{S}(\cdot) : (-\infty, \infty) \mapsto \left(-\frac{\pi}{2}, \frac{\pi}{2}\right), \quad \text{with } \mathcal{S}(\cdot) = \arctan(\cdot) \tag{48}$$

which makes it possible to show the complete bifurcation structure including parameter values tending to infinity. The origin of the $(\mu_{\mathcal{L}}, \mu_{\mathcal{R}})$ parameter plane in Fig. 13 represents an organizing center of the period adding structure (as well as infinitely many intersection points of any two BCB curves in the quadrant $\mu_{\mathcal{L}} > 0$ and $\mu_{\mathcal{R}} > 0$).

Note first that for $a_{\mathcal{L}} > 0$, $a_{\mathcal{R}} > 0$ map (47) can have at most four fixed points, two at each side of the border point. The two fixed points on the left side of $x = 0$, namely

$$\mathcal{O}_{\mathcal{L}}^{1,2} = -\frac{1}{2a_{\mathcal{L}}}(1 \pm \sqrt{1 + 4a_{\mathcal{L}}\mu_{\mathcal{L}}}) \tag{49}$$

appear for $\mu_{\mathcal{L}} < 0$ due to the fold bifurcation for the parameter values belonging to the curve

$$\phi_{\mathcal{L}} = \left\{ (\mu_{\mathcal{L}}, \mu_{\mathcal{R}}) \,\middle|\, \mu_{\mathcal{L}} = -\frac{1}{4a_{\mathcal{L}}} \right\} \tag{50}$$

which corresponds to the vertical line $\mu_{\mathcal{L}} = -\frac{1}{4}$ in Fig. 13. The unstable fixed point $\mathcal{O}_{\mathcal{L}}^1$ persists for all values of $\mu_{\mathcal{L}}$ on the right side of this line, while the stable fixed point $\mathcal{O}_{\mathcal{L}}^2$ undergoes a BCB at

$$\xi_{\mathcal{L}} = \{(\mu_{\mathcal{L}}, \mu_{\mathcal{R}}) \,|\, \mu_{\mathcal{L}} = 0\} \tag{51}$$

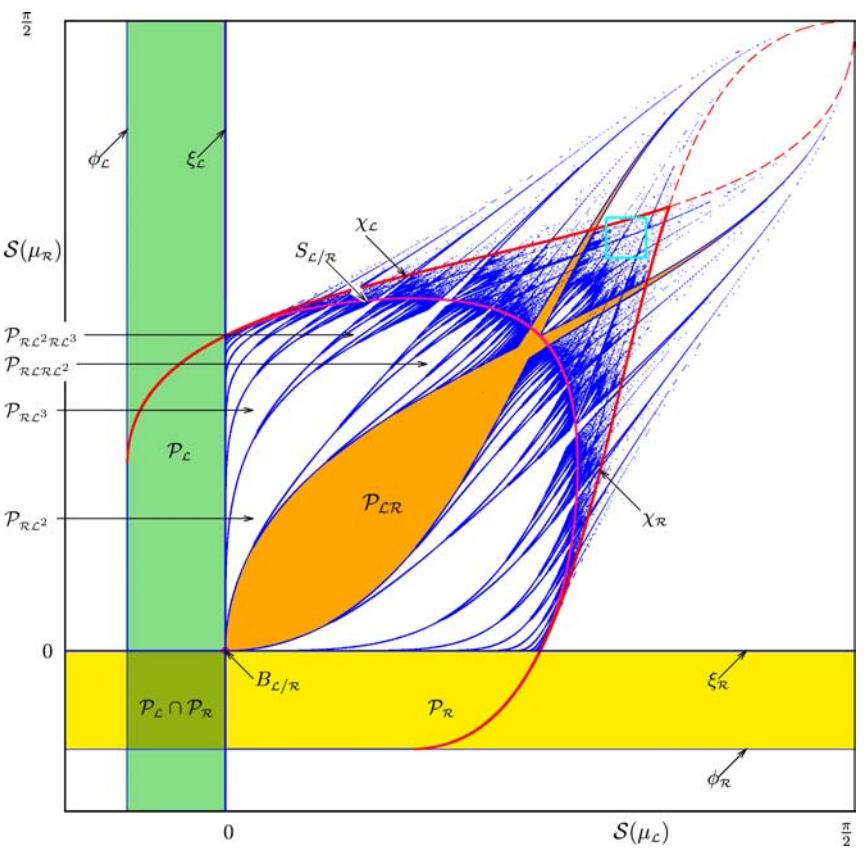


Fig. 13. Bifurcation structure in the $(\mu_{\mathcal{L}}, \mu_{\mathcal{R}})$ parameter plane of the map (47) in the increasing–increasing case ($a_{\mathcal{L}} = a_{\mathcal{R}} = 1$, $\gamma = 2$). The parameters $\mu_{\mathcal{L}}$, $\mu_{\mathcal{R}}$ are shown scaled by the topology-preserving scaling (48). The stability regions of the fixed points $\mathcal{O}_{\mathcal{L}}$, $\mathcal{O}_{\mathcal{R}}$ and of the 2-cycle $\mathcal{O}_{\mathcal{L}\mathcal{R}}$ are marked with $\mathcal{P}_{\mathcal{L}}$, $\mathcal{P}_{\mathcal{R}}$, $\mathcal{P}_{\mathcal{L}\mathcal{R}}$, respectively, and emphasized by colors; some other stability regions are indicated as well. The marked rectangle is shown enlarged in Fig. 14.

and does not exist on the right side of this line. Similarly, we obtain the fold and the BCB curves for the two other fixed points. The fold bifurcation curve at which the fixed points

$$\mathcal{O}_{\mathcal{R}}^{1,2} = -\frac{1}{2a_{\mathcal{R}}}(1 \pm \sqrt{1 + 4a_{\mathcal{R}}\mu_{\mathcal{R}}}) \tag{52}$$

appear, is given by

$$\phi_{\mathcal{R}} = \left\{ (\mu_{\mathcal{L}}, \mu_{\mathcal{R}}) \,\middle|\, \mu_{\mathcal{R}} = -\frac{1}{4a_{\mathcal{R}}} \right\} \tag{53}$$

and for the BCB curve of the stable fixed point $\mathcal{O}_{\mathcal{R}}^{2}$ we get

$$\xi_{\mathcal{R}} = \{(\mu_{\mathcal{L}}, \mu_{\mathcal{R}}) \,|\, \mu_{\mathcal{R}} = 0\}. \tag{54}$$

It can easily be seen that point $\mathcal{B}_{\mathcal{L}/\mathcal{R}} := (\mu_{\mathcal{L}}, \mu_{\mathcal{R}}) = (0, 0)$ is a codimension-2 BCB point at which the function $g$ in (47) is continuous and strictly increasing on both sides of the border point, so that Theorem 1 can be applied. The curves $\xi_{\mathcal{L}}$ and $\xi_{\mathcal{R}}$ which intersect at $\mathcal{B}_{\mathcal{L}/\mathcal{R}}$ are related to the fixed points, hence the first return map, which has to be considered for the description of the bifurcation structure originating from $\mathcal{B}_{\mathcal{L}/\mathcal{R}}$, is given by map (47) itself. Therefore all results stated in Sec. 3.1 for $\tilde{f}$ apply for this map. The attracting cycles whose existence regions originate from the point $\mathcal{B}_{\mathcal{L}/\mathcal{R}}$ and are located in $\mathcal{P}_{\mathcal{B}}$ are as described in Sec. 3.1. In particular, the cycles with the complexity level one are as given by (19). The associated BCB curves are given by Eqs. (20) and (21) with $g_{\mathcal{L}}$, $g_{\mathcal{R}}$ in place of $\tilde{f}_{\mathcal{L}}$, $\tilde{f}_{\mathcal{R}}$, respectively. Similarly, the cycles with complexity level two are as given by (22), and so on for any complexity level.

As shown in Sec. 3.1, the proof of the results stated above refers only to the bifurcation structure in a proper neighborhood of point $\mathcal{B}_{\mathcal{L}/\mathcal{R}}$. Indeed, in this example the results are valid in quite a large part of the parameter plane, namely, in the region bounded by BCB curves $\xi_{\mathcal{L}}$, $\xi_{\mathcal{R}}$ and curve

$$\begin{aligned} S_{\mathcal{L}/\mathcal{R}} &= \{(\mu_{\mathcal{L}}, \mu_{\mathcal{R}}) \,|\, g_{\mathcal{L}} \circ g_{\mathcal{R}}(0) = g_{\mathcal{R}} \circ g_{\mathcal{L}}(0)\} \\ &= \{(\mu_{\mathcal{L}}, \mu_{\mathcal{R}}) \,|\, \mu_{\mathcal{L}} + a_{\mathcal{R}}\mu_{\mathcal{L}}^2 = \mu_{\mathcal{R}} - a_{\mathcal{L}}\mu_{\mathcal{R}}^2\} \end{aligned} \tag{55}$$

issuing from $\mathcal{B}_{\mathcal{L}/\mathcal{R}}$ (although close to $S_{\mathcal{L}/\mathcal{R}}$, besides the BCB curves, fold bifurcation curves of $k$-cycles for any $k > 0$ exist and beyond the stability regions also). The periodicity regions related to cycles of periods larger than 2 of map $g$ have shapes similar to that of the 2-cycle which is highlighted in color in Fig. 13.

In the parameter region bounded by the curves $\xi_{\mathcal{L}}$, $\xi_{\mathcal{R}}$ and $S_{\mathcal{L}/\mathcal{R}}$ map (47) is invertible in the absorbing interval $I = [g_{\mathcal{R}}(0), g_{\mathcal{L}}(0)]$; it is a so-called gap map. Maps of this class have been investigated by many authors (see for example, [Gambaudo *et al.*, 1986; Procaccia *et al.*, 1987; Lyubimov *et al.*, 1989; Homburg, 1996; Berry & Mestel, 1991; Martens & de Melo, 2001; Labarca & Moreira, 2001]). In particular, for a gap map it is proved that the rotation number of an orbit does not depend on the initial point $x \in I$, so that one can refer to the rotation number of the map. It is also known that if the rotation number is rational then possible attractors of the map are attracting cycles only. All these cycles necessarily have the same period[11] [Keener, 1980; Ding & Fan, 1999]. By contrast, if the rotation number of the map is irrational, then the map has a unique Cantor set attractor. An example of a Cantor set attractor in the flow given by Eq. (43), corresponding to the Cantor set attractor of the map $g$, is presented in [Zaks, 1993].

For parameter points located between curve $S_{\mathcal{L}/\mathcal{R}}$ and curves of so-called final bifurcations (related to boundary crises) $\chi_{\mathcal{L}}$ and $\chi_{\mathcal{R}}$ defined by

$$\begin{aligned} \chi_{\mathcal{L}} &= \{(\mu_{\mathcal{L}}, \mu_{\mathcal{R}}) \,|\, g_{\mathcal{R}}(0) = \mathcal{O}_{\mathcal{L}}^{1}\} \\ &= \{(\mu_{\mathcal{L}}, \mu_{\mathcal{R}}) \,|\, \sqrt{1 + 4a_{\mathcal{L}}\mu_{\mathcal{L}}} + 2a_{\mathcal{L}}\mu_{\mathcal{R}} + 1 = 0\} \end{aligned} \tag{56a}$$

$$\begin{aligned} \chi_{\mathcal{R}} &= \{(\mu_{\mathcal{L}}, \mu_{\mathcal{R}}) \,|\, g_{\mathcal{L}}(0) = \mathcal{O}_{\mathcal{R}}^{1}\} \\ &= \{(\mu_{\mathcal{L}}, \mu_{\mathcal{R}}) \,|\, \sqrt{1 + 4a_{\mathcal{R}}\mu_{\mathcal{R}}} + 2a_{\mathcal{R}}\mu_{\mathcal{L}} + 1 = 0\} \end{aligned} \tag{56b}$$

infinitely many other periodicity regions can be observed. As one can see, for example in Fig. 14(a), infinitely many BCB curves bounding the periodicity regions of stable cycles intersect. Each intersection point represents an organizing center of a full period adding structure.

As an example, let us consider such an organizing center shown in Fig. 14(b). It is the intersection point of the BCB curves $\xi_{\mathcal{L}\mathcal{R}^2\mathcal{L}}$ and $\xi_{\mathcal{R}\mathcal{L}^2\mathcal{R}\mathcal{L}}$ of the attracting cycles $\mathcal{O}_{\mathcal{L}\mathcal{R}^2\mathcal{L}}$ and $\mathcal{O}_{\mathcal{R}\mathcal{L}^2\mathcal{R}\mathcal{L}}$ (we have already mentioned that in the case $\gamma > 1$ all the cycles undergoing a BCB are attracting).

[11] In particular this holds for map (47), for which it can also be shown that at most two stable cycles can coexist.

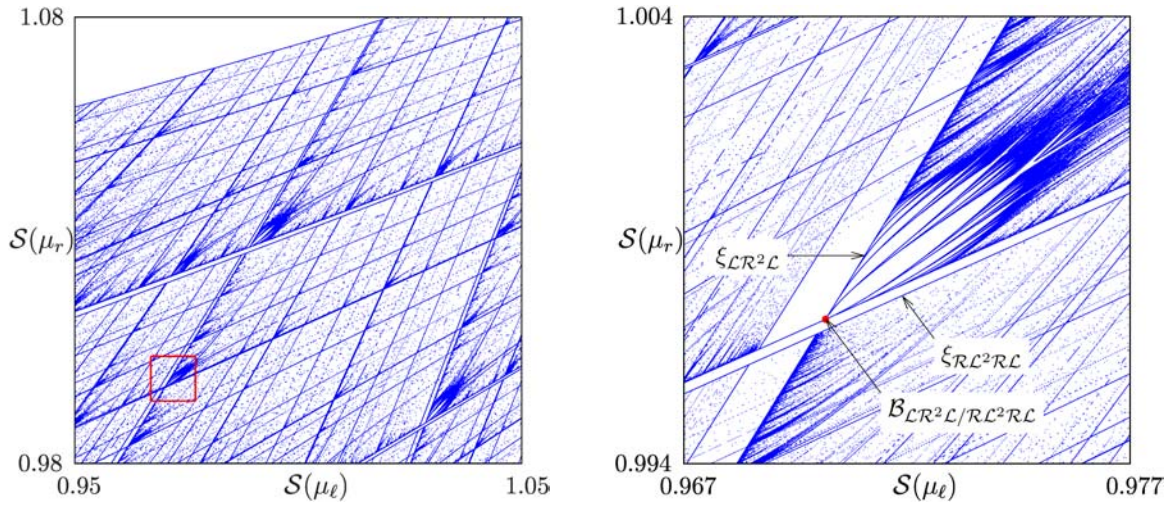


(a) (b)

Fig. 14. Bifurcation structure of the parameter region marked in Fig. 13. The rectangle marked in (a) is shown enlarged in (b).

Accordingly, to describe the periodicity regions originating from this point, denoted in the following as $\mathcal{B}_{\mathcal{LR}^2\mathcal{L}/\mathcal{RL}^2\mathcal{RL}}$, we have to consider the first return map given by

$$x_{n+1} = \tilde{f}(x_n) = \begin{cases} \tilde{f}_{\mathcal{L}}(x_n) \\ \quad = g_{\mathcal{L}} \circ g_{\mathcal{R}}^2 \circ g_{\mathcal{L}}(x_n) & \text{if } x_n < 0 \\ \tilde{f}_{\mathcal{R}}(x_n) \\ \quad = g_{\mathcal{L}} \circ g_{\mathcal{R}} \circ g_{\mathcal{L}}^2 \circ g_{\mathcal{R}}(x_n) & \text{if } x_n > 0. \end{cases} \tag{57}$$

It can also be shown that at the point $\mathcal{B}_{\mathcal{LR}^2\mathcal{L}/\mathcal{RL}^2\mathcal{RL}}$ we have:

$$\begin{aligned} &\frac{d}{dx}\tilde{f}_{\mathcal{L}}\Big|_{x=0} = 0, \quad \frac{d}{dx}\tilde{f}_{\mathcal{R}}\Big|_{x=0} = 0, \\ &\frac{d^2}{dx^2}\tilde{f}_{\mathcal{L}}\Big|_{x=0} \in (0,1), \quad \frac{d^2}{dx^2}\tilde{f}_{\mathcal{R}}\Big|_{x=0} \in (0,1). \end{aligned} \tag{58}$$

Moreover, from the enlargement it can be seen that region $\mathcal{P}_{\mathcal{B}}$ in a neighborhood $U(\mathcal{B})$ is such that an arc connecting a point $A_{\mathcal{L}}$ on the BCB curve $\xi_{\mathcal{LR}^2\mathcal{L}}$ (where $\tilde{f}_{\mathcal{L}}(0) = 0$ and $\tilde{f}_{\mathcal{R}}(0) < 0$) with a point $A_{\mathcal{R}}$ on the BCB curve $\xi_{\mathcal{RL}^2\mathcal{RL}}$ (where $\tilde{f}_{\mathcal{L}}(0) > 0$ and $\tilde{f}_{\mathcal{R}}(0) = 0$) can be chosen in the region where $\mu_{\mathcal{L}}$ is increasing and $(-\mu_{\mathcal{R}})$ is increasing. Thus, if a parameter point $b = (\mu_{\mathcal{L}}, \mu_{\mathcal{R}})$ moves from $\mathcal{A}_{\mathcal{L}}$ to $\mathcal{A}_{\mathcal{R}}$, then for any two points $b_1 = (\mu_{\mathcal{L}}^1, \mu_{\mathcal{R}}^1)$, $b_2 = (\mu_{\mathcal{L}}^2, \mu_{\mathcal{R}}^2)$ such that $b_1$ is passed before $b_2$, we have $\mu_{\mathcal{L}}^1 < \mu_{\mathcal{L}}^2$ so that $\tilde{f}_{\mathcal{L}}(0; b_1) < \tilde{f}_{\mathcal{L}}(0; b_2)$ (as a composition of increasing functions). Similarly, from $-\mu_{\mathcal{R}}^1 < -\mu_{\mathcal{R}}^2$ we have $\tilde{f}_{\mathcal{R}}(0; b_1) < \tilde{f}_{\mathcal{R}}(0; b_2)$. Therefore, the assumptions of Theorem 1 are satisfied, and in the $(\mu_{\mathcal{L}}, \mu_{\mathcal{R}})$ parameter plane the existence regions of the cycles issue from point $\mathcal{B}_{\mathcal{LR}^2\mathcal{L}/\mathcal{RL}^2\mathcal{RL}}$ and organized in the period adding structure. Hence, we can also identify the families of the associated cycles for the original map (47) shown in Fig. 14(b). For example, the families of the cycles with complexity level one are given by

$$\begin{aligned} &\{\mathcal{O}_{\mathcal{RL}^2\mathcal{RL}(\mathcal{LR}^2\mathcal{L})^{n_1}} \,|\, n_1 > 0\}, \\ &\{\mathcal{O}_{\mathcal{LR}^2\mathcal{L}(\mathcal{RL}^2\mathcal{RL})^{n_1}} \,|\, n_1 > 0\} \end{aligned} \tag{59}$$

whose BCB equations are given by Eqs. (20) and (21) with $\tilde{f}_{\mathcal{L}}$ and $\tilde{f}_{\mathcal{R}}$ as defined in Eq. (57), and so on for the higher complexity levels.

Similarly, infinitely many other codimension-2 points which can be seen in Fig. 13 can be dealt with. Further examples for the first return map in the increasing–increasing configuration are commented on in Secs. 4.2 and 4.3.

### 4.2. *Increasing–decreasing case*

Examples for the occurrence of a period incrementing structure on map (47) with $\gamma > 1$, $a_{\mathcal{L}} > 0$, $a_{\mathcal{R}} < 0$ are illustrated in Fig. 15. As in the previous case, the bifurcation structure issuing from the intersection point $\mathcal{B}_{\mathcal{L}/\mathcal{R}} = (0, 0)$ of the BCB curves $\xi_{\mathcal{L}}$ and $\xi_{\mathcal{R}}$ of the fixed points of $g$ can be specified using the function $g$, which is continuous at this

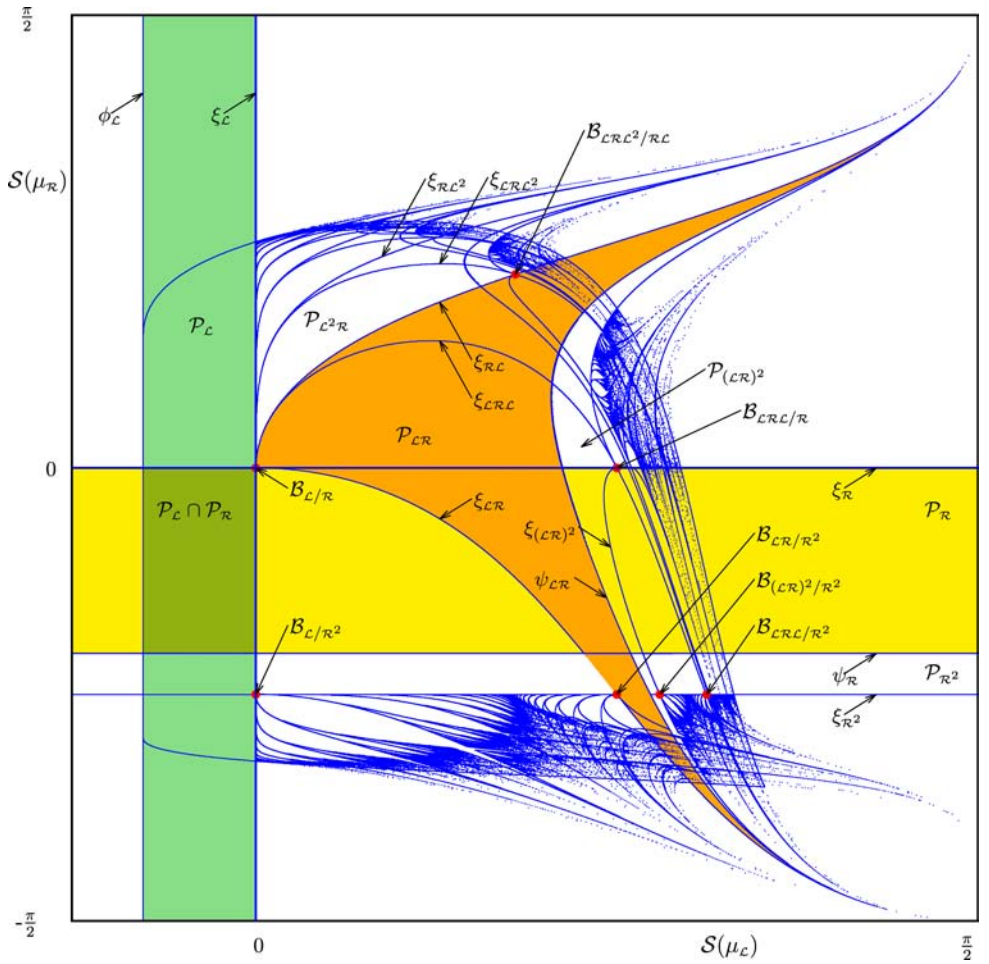


Fig. 15. Bifurcation structure in the $(\mu_\mathcal{L}, \mu_\mathcal{R})$ parameter plane map (47) in the increasing–decreasing case ($a_\mathcal{L} = 1$, $a_\mathcal{R} = -1$, $\gamma = 2$). The parameters $\mu_\mathcal{L}$, $\mu_\mathcal{R}$ are shown scaled by the topology-preserving scaling (48). The stability regions of the fixed points $\mathcal{O}_\mathcal{L}$, $\mathcal{O}_\mathcal{R}$ and of the 2-cycle $\mathcal{O}_{\mathcal{LR}}$ are marked with $\mathcal{P}_\mathcal{L}$, $\mathcal{P}_\mathcal{R}$, $\mathcal{P}_{\mathcal{LR}}$, respectively, and highlighted in color; some other stability regions are marked as well.

point and satisfies

$$\begin{aligned} &\frac{d}{dx} g_\mathcal{L}\Big|_{x=0} = 0, \quad \frac{d}{dx} g_\mathcal{R}\Big|_{x=0} = 0, \\ &\frac{d^2}{dx^2} g_\mathcal{L}\Big|_{x=0} \in (0,1), \quad \frac{d^2}{dx^2} g_\mathcal{R}\Big|_{x=0} \in (-1,0). \end{aligned} \tag{60}$$

Thus, from Theorem 2 (whose assumptions are satisfied) it follows that a period incrementing structure issues from $\mathcal{B}_{\mathcal{L}/\mathcal{R}}$. Accordingly, the family of cycles whose existence regions originate from this point is

$$\{\mathcal{O}_{\mathcal{RL}^n} \,|\, n > 0\}. \tag{61}$$

These regions partially overlap pairwise and accumulate to the BCB curve $\xi_\mathcal{L}$ (the vertical axis). In particular, the lower boundary of region $\mathcal{P}_{\mathcal{LR}}$ is located below curve $\xi_\mathcal{R}$, so that the stable cycle $\mathcal{O}_{\mathcal{LR}}$ coexists with the stable fixed point $\mathcal{O}_\mathcal{R}$ in a proper region.

In Fig. 15 many other organizing centers can be identified. For example, point $\mathcal{B}_{\mathcal{LR}/\mathcal{R}^2}$ represents the issuing point of one more period incrementing structure. To show that one BCB curve is $\xi_{\mathcal{LR}}$, which is the lower boundary of the periodicity region of the attracting 2-cycle $\mathcal{O}_{\mathcal{LR}}$ (highlighted in color in Fig. 15). Then, in the present case, the fixed point $\mathcal{O}_\mathcal{R}$ undergoes a flip bifurcation (instead of a fold) occurring when parameter values belong to the curve

$$\psi_\mathcal{R} = \{(\mu_\mathcal{L}, \mu_\mathcal{R}) \,|\, \sqrt{1 + 4a_\mathcal{R}\mu_\mathcal{R}} - 2 = 0\}. \tag{62}$$

At this bifurcation curve a stable 2-cycle $\mathcal{O}_{\mathcal{R}^2}$ appears (in Fig. 15 the curve $\psi_\mathcal{R}$ corresponds to the horizontal line $\mu_\mathcal{R} = -\frac{1}{4}$). This 2-cycle undergoes a BCB at the parameter values belonging to

the curve given by the condition $g^2_{\mathcal{R}}(0) = 0$, that is

$$\xi_{\mathcal{R}^2} = \left\{ (\mu_{\mathcal{L}}, \mu_{\mathcal{R}}) \,\middle|\, \mu_{\mathcal{R}} = \frac{1}{a_{\mathcal{R}}} \right\} \tag{63}$$

(in our example $\mu_{\mathcal{R}} = -1$). Thus, point $\mathcal{B}_{\mathcal{LR}/\mathcal{R}^2}$ represents an intersection point of BCB curves $\xi_{\mathcal{LR}}$ and $\xi_{\mathcal{R}^2}$. Accordingly, we define the first return map

$$\begin{aligned} x_{n+1} &= \tilde{f}(x_n) \\ &= \begin{cases} \tilde{f}_{\mathcal{L}}(x_n) = g_{\mathcal{R}} \circ g_{\mathcal{L}}(x_n) & \text{if } x_n < 0 \\ \tilde{f}_{\mathcal{R}}(x_n) = g^2_{\mathcal{R}}(x_n) & \text{if } x_n > 0. \end{cases} \end{aligned} \tag{64}$$

Evaluating the second derivatives of $\tilde{f}_{\mathcal{L}}$ and $\tilde{f}_{\mathcal{R}}$ in $x = 0$, from (60) we conclude that in a neighborhood of point $\mathcal{B}_{\mathcal{LR}/\mathcal{R}^2}$ function $\tilde{f}_{\mathcal{L}}$ is strictly decreasing and function $\tilde{f}_{\mathcal{R}}$ is strictly increasing in the left and right neighborhoods of $x = 0$, respectively. This configuration is, as mentioned above, topologically conjugate to the increasing–decreasing one. Regarding the monotonicity of the offsets, the results are obtained from the monotonicity of the functions in the components (here $g_{\mathcal{L}}$ is increasing and $g_{\mathcal{R}}$ is decreasing). If a point $b = (\mu_{\mathcal{L}}, \mu_{\mathcal{R}})$ moves from a point $A_{\mathcal{L}}$ on $\xi_{\mathcal{LR}}$ to a point $\mathcal{A}_{\mathcal{R}}$ on $\xi_{\mathcal{R}^2}$ along an arc $\gamma$ in the region $\mathcal{P}_{\mathcal{R}}$, then for any two points $b_1 = (\mu^1_{\mathcal{L}}, \mu^1_{\mathcal{R}})$ and $b_2 = (\mu^2_{\mathcal{L}}, \mu^2_{\mathcal{R}})$ such that $b_1$ is passed before $b_2$, we have $\mu^1_{\mathcal{L}} > \mu^2_{\mathcal{L}}$ and $\mu^1_{\mathcal{R}} < \mu^2_{\mathcal{R}}$. Thus, for the left offset we have to show that $\tilde{f}_{\mathcal{L}}(0, b_1) < \tilde{f}_{\mathcal{L}}(0, b_2)$. In fact, by definition of $\tilde{f}_{\mathcal{L}}$ we have $\tilde{f}_{\mathcal{L}}(0, b_1) = \mu^1_{\mathcal{L}} > \tilde{f}_{\mathcal{L}}(0, b_1) = \mu^2_{\mathcal{L}}$ and hence $g_{\mathcal{R}}(g_{\mathcal{L}}(0, b_1)) = g_{\mathcal{R}}(\mu^1_{\mathcal{L}}, b_1) < g_{\mathcal{R}}(g_{\mathcal{L}}(0, b_2)) = g_{\mathcal{R}}(\mu^2_{\mathcal{L}}, b_2)$. Similarly, for the right offset we have to show that $\tilde{f}_{\mathcal{R}}(0, b_1) < \tilde{f}_{\mathcal{R}}(0; b_2)$. Indeed, by definition of $\tilde{f}_{\mathcal{R}}$ we have $\tilde{f}_{\mathcal{R}}(0, b_1) = -\mu^1_{\mathcal{R}} > \tilde{f}_{\mathcal{R}}(0, b_1) = -\mu^2_{\mathcal{R}}$ and hence $f_{\mathcal{R}}(f_{\mathcal{R}}(0, b_1)) = f_{\mathcal{R}}(-\mu^1_{\mathcal{L}}, b_1) < f_{\mathcal{R}}(f_{\mathcal{L}}(0, b_2)) = f_{\mathcal{R}}(-\mu^2_{\mathcal{L}}, b_2)$. Note that similar reasoning can be applied in all the other examples of codimension-2 points. Thus, the monotonicity of the offsets is a consequence of the monotonicity of the functions defining the first return map. Therefore, for the first return map (64) there exists the family of cycles

$$\{\tilde{\mathcal{O}}_{\mathcal{LR}^n} \,|\, n > 0\} \tag{65}$$

whose existence regions issue from $\mathcal{B}_{\mathcal{LR}/\mathcal{R}^2}$. The boundaries of these regions are the BCB curves given by Eq. (21) with $n_1 = n$, and with $\tilde{f}_{\mathcal{L}}$ and $\tilde{f}_{\mathcal{R}}$ defined as in (64). The family of cycles for the original map (47) is given by the cycles with symbolic sequences $(\mathcal{LR})(\mathcal{R}^2)^n$, that is

$$\{\mathcal{O}_{\mathcal{LR}^{2n+1}} \,|\, n > 0\}. \tag{66}$$

The related existence regions $\mathcal{P}_{\mathcal{LR}^{2n+1}}$ form the period incrementing structure originating from point $\mathcal{B}_{\mathcal{LR}/\mathcal{R}^2}$ and for each $n$ the pair of regions $\mathcal{P}_{\mathcal{LR}^{2n+1}}$ and $\mathcal{P}_{\mathcal{LR}^{2n+3}}$ partially overlap.

The same reasoning applies to the intersection point of the BCB curve $\xi_{\mathcal{R}^2}$ not only with $\xi_{\mathcal{LR}}$, but also with any of the curves $\xi_{\mathcal{LRL}^{k-1}}$ for $k > 1$. These BCB curves represent the lower boundaries of the existence regions of the cycles $\mathcal{O}_{\mathcal{L}^k\mathcal{R}}$, which emerge at point $\mathcal{B}_{\mathcal{L}/\mathcal{R}}$. In fact, at the intersection point $\mathcal{B}_{\mathcal{LRL}^{k-1}/\mathcal{R}^2}$ the corresponding first return map

$$\begin{aligned} x_{n+1} &= \tilde{f}(x_n) \\ &= \begin{cases} \tilde{f}_{\mathcal{L}}(x_n) = g^{k-1}_{\mathcal{L}} \circ g_{\mathcal{R}} \circ g_{\mathcal{L}}(x_n) & \text{if } x_n < 0 \\ \tilde{f}_{\mathcal{R}}(x_n) = g^2_{\mathcal{R}}(x_n) & \text{if } x_n > 0 \end{cases} \end{aligned} \tag{67}$$

is in the decreasing–increasing configuration. Therefore, along the line $\xi_{\mathcal{R}^2}$ we observe an infinite sequence of organizing centers $\mathcal{B}_{\mathcal{LRL}^{k-1}/\mathcal{R}^2}$, from each of which a period incrementing structure is issuing. Points $\mathcal{B}_{\mathcal{LR}/\mathcal{R}^2}$ and $\mathcal{B}_{\mathcal{LRL}/\mathcal{R}^2}$ marked in Fig. 15 belong to this family corresponding to cases $k = 1$ and $k = 2$, respectively. The period incrementing structure issuing from point $\mathcal{B}_{\mathcal{LRL}^{k-1}/\mathcal{R}^2}$ is formed by the pairwise overlapping regions associated with the cycles from the family

$$\{\mathcal{O}_{\mathcal{LRL}^{k-1}\mathcal{R}^{2n}} \,|\, n > 0\} \tag{68}$$

whose BCB curves are given by Eq. (21) with $n_1 = n$, and with $\tilde{f}_{\mathcal{L}}$ and $\tilde{f}_{\mathcal{R}}$ defined as in Eq. (67).

It is also clearly visible in Fig. 15 that not all the organizing centers in the $(\mu_{\mathcal{L}}, \mu_{\mathcal{R}})$ plane are associated with period incrementing structures. For example, point $\mathcal{B}_{\mathcal{L}/\mathcal{R}^2} \in \xi_{\mathcal{L}} \cap \xi_{\mathcal{R}^2} = (0, -1)$ gives rise to a period adding structure. It can easily be shown that at this point the first return map

$$\begin{aligned} x_{n+1} &= \tilde{f}(x_n) \\ &= \begin{cases} \tilde{f}_{\mathcal{L}}(x_n) = g_{\mathcal{L}}(x_n) & \text{if } x_n < 0 \\ \tilde{f}_{\mathcal{R}}(x_n) = g^2_{\mathcal{R}}(x_n) & \text{if } x_n > 0 \end{cases} \end{aligned} \tag{69}$$

is in the increasing–increasing configuration and the offsets $\tilde{f}_{\mathcal{L}}(0)$, $\tilde{f}_{\mathcal{R}}(0)$ are increasing when the parameters are moved along an arc $\gamma$ in region $\mathcal{P}_{\mathcal{B}}$. Therefore, for this map we can guarantee the existence of cycles of all the complexity levels whose existence

regions are organized in the period adding structure issuing from point $\mathcal{B}_{\mathcal{L}/\mathcal{R}^2}$. A few BCB curves related to the first and the second complexity levels are given in Eqs. (20), (21), (23), (24) with $\tilde{f}_{\mathcal{L}}$ and $\tilde{f}_{\mathcal{R}}$ defined as in Eq. (69).

There are also infinitely many other codimension-2 BCB points located at curve $\xi_{\mathcal{R}^2}$, which lead to the appearance of period adding structures. This can easily be explained taking into account that each of the cycles $\mathcal{O}_{\mathcal{L}^n\mathcal{R}}$ emerging at point $\mathcal{B}_{\mathcal{L}/\mathcal{R}}$ undergoes a flip bifurcation at the curve $\psi_{\mathcal{L}^n\mathcal{R}}$ at which a stable cycle $\mathcal{O}_{(\mathcal{L}^n\mathcal{R})^2}$ of double period emerges. For example, in Fig. 15 the flip bifurcation curve $\psi_{\mathcal{LR}}$ is marked, at which the stable cycle $\mathcal{O}_{(\mathcal{LR})^2}$ appears. This cycle undergoes a BCB at curve $\xi_{(\mathcal{LR})^2}$, and the intersection point of this curve with curve $\xi_{\mathcal{R}^2}$ represents the organizing center $\mathcal{B}_{(\mathcal{LR})^2/\mathcal{R}^2}$ which is marked in Fig. 15. It can be shown that the configuration of the associated first return map at this point is increasing–increasing, and the offsets are increasing as well, so that this is an organizing center giving rise to a period adding structure. The same reasoning applies to the cycle $\mathcal{O}_{(\mathcal{L}^n\mathcal{R})^2}$ for any $n$, so that all the intersection points $\mathcal{B}_{(\mathcal{L}^n\mathcal{R})^2/\mathcal{R}^2}$ of the bifurcation curves $\xi_{\mathcal{R}^2}$ and $\xi_{(\mathcal{L}^n\mathcal{R})^2}$ are organizing centers of period adding structures.

### 4.3. *Decreasing–decreasing case*

The structure of the parameter plane of map (47) for $\gamma > 1$, $a_{\mathcal{L}} < 0$, $a_{\mathcal{R}} < 0$ is shown in Fig. 16. As one can see in this figure, the only periodicity region emerging at the origin of the $(\mu_{\mathcal{L}}, \mu_{\mathcal{R}})$ parameter plane is related to the 2-cycle $\mathcal{O}_{\mathcal{LR}}$. Indeed, for $\mu_{\mathcal{L}} > 0$, $\mu_{\mathcal{R}} > 0$ this 2-cycle represents the only possible attractor of map (47). Besides the two BCB curves $\xi_{\mathcal{LR}}$, $\xi_{\mathcal{RL}}$ issuing from the point $\mathcal{B}_{\mathcal{L}/\mathcal{R}} = (0, 0)$ its existence region is bounded by a fold bifurcation curve $\phi_{\mathcal{LR}}$.

One more example of the coupling bifurcation structure of the colliding cycles can be seen in

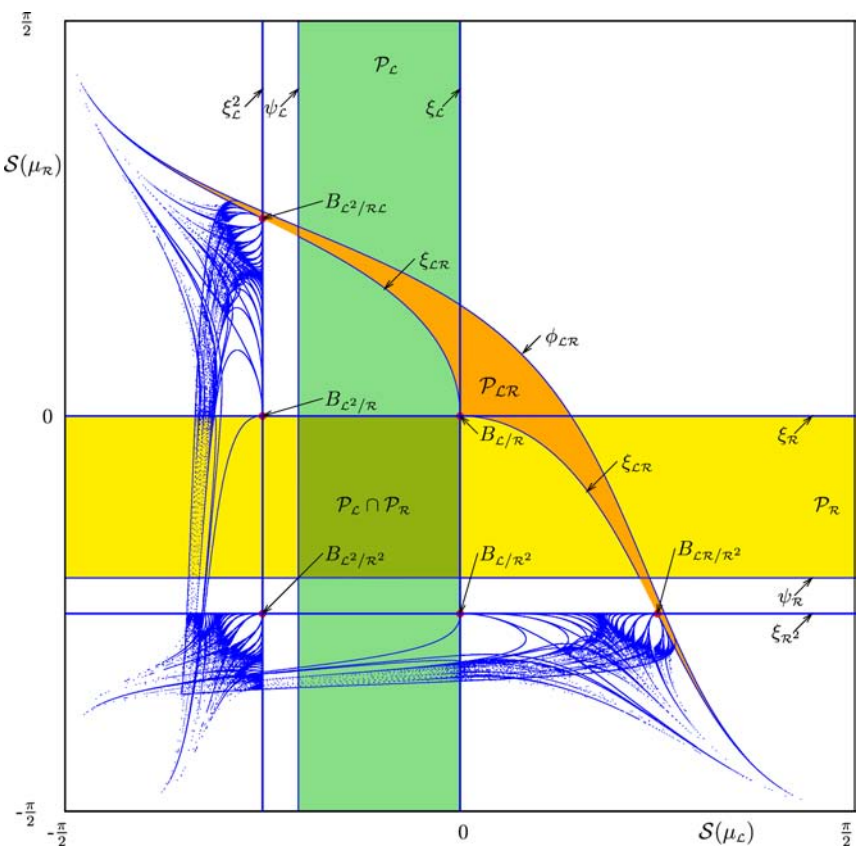


Fig. 16. Bifurcation structure in the $(\mu_{\mathcal{L}}, \mu_{\mathcal{R}})$ parameter plane of map (47) in the decreasing–decreasing case ($a_{\mathcal{L}} = a_{\mathcal{R}} = -1$, $\gamma = 2$). The parameters $\mu_{\mathcal{L}}$, $\mu_{\mathcal{R}}$ are shown scaled by the topology-preserving scaling (48). The stability regions of the fixed points $\mathcal{O}_{\mathcal{L}}$, $\mathcal{O}_{\mathcal{R}}$ and of the 2-cycle $\mathcal{O}_{\mathcal{LR}}$ are marked with $\mathcal{P}_{\mathcal{L}}$, $\mathcal{P}_{\mathcal{R}}$, $\mathcal{P}_{\mathcal{LR}}$, respectively, and highlighted in colors. Region $\mathcal{P}_{\mathcal{LR}}$ is also bounded by the fold bifurcation curve $\phi_{\mathcal{LR}}$.

Fig. 15. In fact, $\mathcal{B}_{\mathcal{LRL}/\mathcal{R}}$ represents the intersection point of the BCB curves $\xi_{\mathcal{LRL}}$ (the lower boundary of the existence region of the stable 3-cycle $\mathcal{O}_{\mathcal{L}^2\mathcal{R}}$) and $\xi_{\mathcal{R}}$ (the upper boundary of the existence region of the stable fixed point $\mathcal{O}_{\mathcal{R}}$). At this point we can verify that the first return map defined by

$$x_{n+1} = \tilde{f}(x_n) = \begin{cases} \tilde{f}_{\mathcal{L}}(x_n) = g_{\mathcal{L}} \circ g_{\mathcal{R}} \circ g_{\mathcal{L}}(x_n) & \text{if } x_n < 0 \\ \tilde{f}_{\mathcal{R}}(x_n) = g_{\mathcal{R}}(x_n) & \text{if } x_n > 0 \end{cases} \tag{70}$$

is in the decreasing–decreasing configuration, and an arc connecting the two boundaries in the region $\mathcal{P}_{\mathcal{B}}$ can be chosen such that $\mu_{\mathcal{L}}$ is increasing and $(-\mu_{\mathcal{R}})$ is increasing, thus the offsets $\tilde{f}_{\mathcal{L}}(0)$ and $\tilde{f}_{\mathcal{R}}(0)$ are increasing along this arc. Therefore, the only periodicity region which emerges at point $\mathcal{B}_{\mathcal{LRL}/R}$ is the one related to the 2-cycle $\tilde{\mathcal{O}}_{\mathcal{LR}}$ of map (70). Clearly, this coupled 2-cycle corresponds to the 4-cycle $\tilde{\mathcal{O}}_{(\mathcal{LR})^2}$ of the original map (47), whose existence region partially overlaps with the regions of the two colliding cycles, leading to bistability.

Similar reasoning can be applied to explain the bifurcation structure shown in Fig. 15 at infinitely many other codimension-2 BCB points. In fact, considering the periodicity regions related to the family of cycles $\mathcal{O}_{\mathcal{L}^k\mathcal{R}}$, which emerge at the point $\mathcal{B}_{\mathcal{L}/\mathcal{R}}$, it can be shown that for each $k$ the BCB curves $\xi_{\mathcal{LRL}^k}$ (the lower boundary of the existence region of the $(k+2)$-cycle $\mathcal{O}_{\mathcal{L}^{k+1}\mathcal{R}}$) and $\xi_{\mathcal{RL}^{k-1}}$ (the upper boundary of the existence region of the $k$-cycle $\mathcal{O}_{\mathcal{RL}^{k-1}}$) intersect. At intersection point $\mathcal{B}_{\mathcal{LRL}^k/\mathcal{RL}^{k-1}}$ the related first return map is given by

$$x_{n+1} = \tilde{f}(x_n) = \begin{cases} \tilde{f}_{\mathcal{L}}(x_n) = g_{\mathcal{L}}^k \circ g_{\mathcal{R}} \circ g_{\mathcal{L}}(x_n) & \text{if } x_n < 0 \\ \tilde{f}_{\mathcal{R}}(x_n) = g_{\mathcal{L}}^k \circ g_{\mathcal{R}}(x_n) & \text{if } x_n > 0 \end{cases} \tag{71}$$

and it is in the decreasing–decreasing configuration. Accordingly, from point $\mathcal{B}_{\mathcal{LRL}^k/\mathcal{RL}^{k-1}}$ the region of the coupled 2-cycle $\tilde{\mathcal{O}}_{\mathcal{LR}}$ of map (71) is issuing, which corresponds to the $2(k+1)$-cycle of map (47) with the symbolic sequence $\mathcal{LRL}^k\mathcal{RL}^{k-1} \equiv (\mathcal{L}^k\mathcal{R})^2$. As in the previous example, for each $k$ the existence region of this cycle partially overlaps with the regions of the colliding cycles. Besides these curves, each region is also bounded by the flip bifurcation curve $\psi_{\mathcal{L}^k\mathcal{R}}$ of the corresponding $(k+1)$-cycle $\mathcal{O}_{\mathcal{L}^k\mathcal{R}}$ which belongs to the family emerging at point $\mathcal{B}_{\mathcal{L}/R}$.

To conclude, let us comment on a few more codimension-2 BCB points which can be observed in map (47) in the decreasing–decreasing configuration as shown in Fig. 16. By contrast to the first quadrant, in which there is only one stability region $\mathcal{P}_{\mathcal{LR}}$, if at least one of the offsets $\mu_{\mathcal{L}}$, $\mu_{\mathcal{R}}$ is negative, other attracting cycles appear, and their existence regions originate from several organizing centers given by codimension-2 BCB points. In particular, we observe points $\mathcal{B}_{\mathcal{L}/\mathcal{R}^2}$ and $\mathcal{B}_{\mathcal{LR}/\mathcal{R}^2}$ as in Fig. 15. As before, their appearance is caused by the intersection of BCB curve $\xi_{\mathcal{R}^2}$ with BCB curves $\xi_{\mathcal{L}}$ and $\xi_{\mathcal{LR}}$, respectively (cf. Figs. 15 and 16). What differs with respect to the previous case are the shapes of the first return maps (69) and (67) at these points. Recall that in the case of Fig. 15 the first return map (69) is in the increasing–increasing configuration at point $\mathcal{B}_{\mathcal{L}/\mathcal{R}^2}$, and, accordingly, this point represents the issuing point of a period adding structure. Now, in Fig. 16, the first return map (69) is in the increasing–decreasing configuration at point $\mathcal{B}_{\mathcal{L}/\mathcal{R}^2}$. Therefore, the period incrementing bifurcation structure is issuing from this point, formed by a family of pairwise overlapping periodicity regions of cycles with symbolic sequences $\mathcal{L}(\mathcal{R}^2)^n$, $n > 0$. Similarly, we can show (by evaluating the corresponding derivatives) that the point $\mathcal{B}_{\mathcal{LR}/\mathcal{R}^2}$, which is the organizing center of a period incrementing structure in Fig. 15, represents now, in Fig. 16, the organizing center of a period adding structure.

In addition to the codimension-2 BCBs points $\mathcal{B}_{\mathcal{L}/\mathcal{R}^2}$ and $\mathcal{B}_{\mathcal{LR}/\mathcal{R}^2}$, in Fig. 16 we can also observe the organizing centers $\mathcal{B}_{\mathcal{L}^2/\mathcal{R}}$ and $\mathcal{B}_{\mathcal{L}^2/\mathcal{RL}}$ of the period incrementing and period adding structure, respectively. Similarly, we can show that point $\mathcal{B}_{\mathcal{L}^2/\mathcal{R}^2} \in \xi_{\mathcal{L}^2} \cap \xi_{\mathcal{R}^2}$ (at which the first return map defined by the branches $\tilde{f}_{\mathcal{L}} = g_{\mathcal{L}}^2$, $\tilde{f}_{\mathcal{R}} = g_{\mathcal{R}}^2$ is in the increasing–increasing configuration) represents the organizing center of a period adding structure.

## 5. Conclusions

In this work we have considered a two-parameter family of 1D piecewise smooth maps with a single discontinuity point $x = 0$. We have investigated the bifurcation structures in a parameter plane, associated with a codimension-2 bifurcation point $\mathcal{B}_{\sigma/\varrho}$,

given by the transverse intersection of two BCB curves associated with attracting cycles. It is worth emphasizing that these bifurcation curves may be related to cycles of any period and any symbolic sequence. We have described in Sec. 3 three different cases associated with the different local monotonicity of the functions. The result of the bifurcation mainly depends on whether at the codimension-2 BCB point the related continuous first return map in a neighborhood of point $x = 0$ is increasing or decreasing in a right and a left neighborhood of $x = 0$. We have shown that if the first return map is strictly increasing on both sides of $x = 0$ then a *full period adding bifurcation structure* is issuing from $\mathcal{B}_{\sigma/\varrho}$. If the first return map is strictly increasing on one side of $x = 0$ and strictly decreasing on the other side, then a *period incrementing bifurcation structure* is issuing from $\mathcal{B}_{\sigma/\varrho}$. In these cases point $\mathcal{B}_{\sigma/\varrho}$ is an organizing center. When the first return map is strictly decreasing on both sides of $x = 0$ then only two BCB curves issue from $\mathcal{B}_{\sigma/\varrho}$, bounding the region of existence of *a cycle obtained by coupling* the two colliding ones, whose symbolic sequence $\sigma\varrho$ is the concatenation of the symbolic sequences of the two colliding cycles. The existence region of such a coupled cycle partially overlaps with the existence regions of each colliding cycle. In Sec. 4 we have shown how the considered class of maps is associated with Lorenz-like flows possessing a butterfly structure. Such a codimension-2 BCB point in a map associated with a Lorenz-like flow corresponds to the merging (or gluing) of two attracting homoclinic orbits of the flow having any number of loops. We proved that the three theorems apply to all the codimension-2 BCB points existing in the parameter plane of the offsets of the original map.

## Acknowledgments

This work has been carries out within the activity of the PRIN 2009 project "Local interactions and global dynamics in economics and finance: models and tools", MIUR, Italy, and under the auspices of COST Action IS1104 "The EU in the new complex geography of economic systems: models, tools and policy evaluation". The work was also partially supported by the European Community within the scope of the project "Multiple-discontinuity induced bifurcations in theory and applications" (Marie Curie Action of the 7th Framework Programme), and by the German Research Foundation within the scope of the project "Organizing centers in discontinuous dynamical systems: bifurcations of higher codimension in theory and applications".

## References

Apostol, T. [1990] *Modular Functions and Dirichlet Series in Number Theory*, 2nd edition (Springer, NY).

Avrutin, V. & Schanz, M. [2006] "On multi-parametric bifurcations in a scalar piecewise-linear map," *Nonlinearity* **19**, 531–552.

Avrutin, V., Schanz, M. & Banerjee, S. [2006] "Multi-parametric bifurcations in a piecewise-linear discontinuous map," *Nonlinearity* **19**, 1875–1906.

Avrutin, V., Schanz, M. & Banerjee, S. [2007] "Codimension-3 bifurcations: Explanation of the complex 1-, 2- and 3D bifurcation structures in nonsmooth maps," *Phys. Rev. E* **75**, 066205-1–7.

Avrutin, V., Schanz, M. & Gardini, L. [2010] "Calculation of bifurcation curves by map replacement," *Int. J. Bifurcation and Chaos* **20**, 3105–3135.

Avrutin, V., Granados, A. & Schanz, M. [2011] "Sufficient conditions for a period increment big bang bifurcation in one-dimensional maps," *Nonlinearity* **24**, 2575–2598.

Avrutin, V., Schanz, M. & Schenke, B. [2012] "Breaking the continuity of a piecewise linear map," *ESAIM: Proc.* **36**, 73–105.

Berry, D. & Mestel, B. [1991] "Wandering interval for Lorenz maps with bounded nonlinearity," *Bull. London Math. Soc.* **23**, 183–189.

Birman, J. S. & Williams, R. F. [1983] "Knotted periodic orbits in dynamical systems-I: Lorenz's equations," *Topology* **22**, 47–82.

di Bernardo, M., Feigin, M. I., Hogan, S. J. & Homer, M. E. [1999] "Local analysis of C-bifurcations in $n$-dimensional piecewise smooth dynamical systems," *Chaos Solit. Fract.* **10**, 1881–1908.

Ding, Y. & Fan, W. [1999] "The asymptotic periodicity of Lorenz maps," *Acta Math. Sci.* **19**, 114–120.

Gambaudo, J. M., Procaccia, I., Thomae, S. & Tresser, C. [1986] "New universal scenarios for the onset of chaos in Lorenz-type flows," *Phys. Rev. Lett.* **57**, 925–928.

Gambaudo, J. M., Glendinning, P. & Tresser, T. [1988] "The gluing bifurcation: Symbolic dynamics of the closed curves," *Nonlinearity* **1**, 203–214.

Gardini, L. & Tramontana, F. [2010] "Border collision bifurcations in 1D PWL map with one discontinuity and negative jump. Use of the first return map," *Int. J. Bifurcation and Chaos* **20**, 3529–3547.

Gardini, L., Tramontana, F., Avrutin, V. & Schanz, M. [2010] "Border collision bifurcations in 1D piecewise-linear maps and Leonov's approach," *Int. J. Bifurcation and Chaos* **20**, 3085–3104.

Gardini, L. & Tramontana, F. [2011] "Border collision bifurcation curves and their classification in a family of one-dimensional discontinuous maps," *Chaos Solit. Fract.* **44**, 248–259.

Gardini, L., Avrutin, V., Schanz, M., Granados, A. & Sushko, I. [2012] "Organizing centers in parameter space of discontinuous 1d maps. The case of increasing/decreasing branches," *ESAIM: Proc.* **36**, 106–120.

Ghrist, R. & Holmes, P. J. [1993] "Knots and orbit genealogies in three dimensional flows," *Bifurcations and Periodic Orbits of Vector Fields*, ed. Schlomiuk, D. (Kluwer Academic Publishers), pp. 185–239.

Ghrist, R. & Holmes, P. J. [1994] "Knotting within the gluing bifurcation," *IUTAM Symp. Nonlinearity and Chaos in the Engineering Dynamics*, eds. Thompson, J. & Bishop, S. (John Wiley Press), pp. 299–315.

Ghrist, R. [2000] "Resonant gluing bifurcations," *Int. J. Bifurcation and Chaos* **10**, 2141–2160.

Glendinning, P. [1988] "Global bifurcations in flows," *New Directions in Dynamical Systems*, *J. London Math. Soc. Lecture Note Ser.*, eds. Bedford, T. & Swift, J. (Cambridge University Press), pp. 120–149.

Golmakani, A. & Homburg, A. J. [2011] "Lorenz attractors in unfoldings of homoclinic flip bifurcations," *Dyn. Syst.* **26**, 61–76.

Guckenheimer, J. & Williams, R. F. [1979] "Structural stability of Lorenz attractors," *Publ. Math. IHES* **50**, 307–320.

Hardy, G. & Wright, E. [1960] *An Introduction to the Theory of Numbers*, 4th edition (Oxford University Press, London).

Homburg, A. J. [1993] "Some global aspects of homoclinic bifurcations of vector fields," PhD thesis, Rijksuniversiteit Groningen.

Homburg, A. J. [1996] *Global Aspects of Homoclinic Bifurcations of Vector Fields*, Memoirs of the American Math. Soc., Vol. 121.

Keener, J. P. [1980] "Chaotic behavior in piecewise continuous difference equations," *Trans. Am. Math. Soc.* **261**, 589–604.

Labarca, R. & Moreira, C. [2001] "Bifurcation on the essential dynamics of Lorenz maps and applications to Lorenz-like flows: Contributions to study of expanding case," *Bol. Soc. Bras. Mat.* **32**, 107–144.

Labarca, R. & Moreira, C. [2006] "Essential dynamics for Lorenz maps on the real line and the lexicographical world," *Ann. I.H. Poincaré* **AN 23**.

Labarca, R. & Moreira, C. [2010] "Bifurcation of the essential dynamics of Lorenz maps on the real line and the bifurcation scenario for Lorenz like flows: The contracting case," *Proyecciones J. Math.* **29**, 247–293.

Labarca, R. & Vásquez, L. [2012] "A characterization of the kneading sequences associated to Lorenz maps of the interval," *Bull. Braz. Math. Soc.* **43**, 221–245.

Leonov, N. N. [1959] "On a pointwise mapping of a line into itself," *Radiofisika* **2**, 942–956 (in Russian).

Lorenz, E. N. [1963] "Deterministic non-periodic flows," *J. Atmos. Sci.* **20**, 130.

Lyubimov, D. V., Pikovsky, A. S. & Zaks, M. A. [1989] *Universal Scenarios of Transitions to Chaos via Homoclinic Bifurcations*, Math. Phys. Rev., Vol. 8 (Harwood Academic, London), Russian version 1986 as a Preprint (192) of Russian Academy of Science, Institute of Mechanics of Solid Matter, Sverdlovsk.

Martens, M. & de Melo, W. [2001] "Universal models for Lorenz maps," *Ergod. Th. Dyn. Syst.* **21**, 833–860.

Nusse, H. E. & Yorke, J. A. [1992] "Border-collision bifurcations including 'period two to period three' bifurcation for piecewise smooth systems," *Physica D* **57**, 39–57.

Procaccia, I., Thomae, S. & Tresser, C. [1987] "First-return maps as a unified renormalization scheme for dynamical systems," *Phys. Rev. A* **35**, 1884–1900.

Sparrow, C. [1982] *The Lorenz Equations*: *Bifurcations*, *Chaos*, *and Strange Attractors* (Springer-Verlag).

Tramontana, F., Gardini, L., Avrutin, V. & Schanz, M. [2012] "New adding phenomena in piecewise linear maps with two discontinuities," *Int. J. Bifurcation and Chaos* **22**, 1250068.

Turaev, D. V. & Shil'nikov, L. P. [1987 (Russian version 1986)] "On bifurcations of a homoclinic 'Figure of Eight' for a saddle with a negative saddle value," *Soviet Math. Dokl.* **34**, 397–401.

Winckler, B. [2011] "Renormalization of Lorenz maps," PhD thesis, KTH, School of Engineering Sciences.

Zaks, M. A. [1993] "Scaling properties and renormalization invariants for the 'homoclinic quasiperiodicity'," *Physica D* **62**, 300–316.